



POLITECNICO
MILANO 1863

SCUOLA DI INGEGNERIA INDUSTRIALE
E DELL'INFORMAZIONE

Modelling atrial and ventricular
hiPSC cardiomyocytes microtissues
within a 3D beating organ on a chip:
a mechanical, electrical and
biological characterization study

BIOMEDICAL ENGINEERING MASTER THESIS

Author: **Bortolotti Andrea Enrico**

Student ID: 995423

Advisor: Paola Occhetta

Co-advisor: Alessandro Cacioppo

Rodrigo Torres Garcia

Caterina Pernici

Academic Year: 2023-24

Abstract

Globally, cardiovascular diseases (CVDs) are a significant cause of death, accounting for approximately 30% of all fatalities. These conditions involve issues with the vascular, cardiac, and nervous systems. The urgent need for new and improved medications and therapies to reduce the global burden of CVDs is paramount. Being the process of drug development very expensive and time-consuming before they can be brought to market, a new innovative technology has emerged. This technology, called heart on a chip, offering an in vitro model able to recreate an in vivo-like environment useful to drug screening testing. In particular, the combination of 3D structured models with mechanical or electrical stimulation can enhance cell maturation. This model has the potential to enhance cell maturation and provide more consistent outcomes in drug development. This study, carried out in partnership with BiomimX s.r.l., employed a 3D heart-on-a-chip platform to examine the mechanical, electrical, and biological characteristics of atrial and ventricular hiPSC cardiomyocytes. In this way is possible to make a reliable benchmark useful for further drug screening testing. This project is working towards establishing a dependable standard for evaluating the efficacy of new medications for heart conditions. The final goal is to introduce a novel chip design that allows for the simultaneous culture of atrial and ventricular heart cells, addressing past challenges. This innovative method has the potential to significantly shape the fields of cardiac research and drug advancement.

Key-words: Heart-on-a-chip, drug screening, atrial cardiomyocytes, ventricular cardiomyocytes, cardiovascular diseases

Abstract in Italiano

Globalmente, le malattie cardiovascolari (CVD) sono una causa significativa di morte, rappresentando circa il 30% di tutte le fatalità. Queste condizioni coinvolgono problemi con i sistemi vascolare, cardiaco e nervoso. La necessità urgente di nuovi e migliorati farmaci e terapie per ridurre il peso globale delle CVD è fondamentale. Essendo il processo di sviluppo dei farmaci molto costoso e lungo prima che possano essere portati sul mercato, è emersa una nuova tecnologia innovativa. Questa tecnologia, chiamata cuore su un chip, offre un modello in vitro in grado di ricreare un ambiente simile a quello in vivo utile per i test di screening dei farmaci. In particolare, la combinazione di modelli strutturati in 3D con stimolazione meccanica o elettrica può migliorare la maturazione cellulare. Questo modello ha il potenziale per migliorare la maturazione cellulare e fornire risultati più consistenti nello sviluppo dei farmaci. Questo studio, condotto in collaborazione con BiomimX s.r.l., ha impiegato una piattaforma cuore su un chip in 3D per esaminare le caratteristiche meccaniche, elettriche e biologiche dei cardiomiociti atriali e ventricolari hiPSC. In questo modo è possibile creare un punto di riferimento affidabile utile per ulteriori test di screening dei farmaci. Questo progetto si sta impegnando per stabilire uno standard affidabile per valutare l'efficacia dei nuovi farmaci per le condizioni cardiache. L'obiettivo finale è introdurre un nuovo design di chip che consenta la coltura simultanea di cellule cardiache atriali e ventricolari, affrontando sfide passate. Questo metodo innovativo ha il potenziale per plasmare significativamente i campi della ricerca cardiaca e dello sviluppo dei farmaci.

Parole chiave: cuore su chip, screening farmacologico, cardiomiociti atriali, cardiomiociti ventricolari, malattie cardiovascolari

Contents

Abstract	i
Abstract in Italiano	iii
Contents	v
1 Introduction.....	1
2 Materials and methods.....	11
2.1. uHeart on chip.....	11
2.1.1. Microfluidic platform design.....	11
2.1.2. Microfluidic device fabrication	13
2.1.2.1. Microfluidic device assembling	15
2.1.2.2. Microfluidic device testing.....	15
2.1.2.3. Electrodes fabrication and testing	16
2.2. Device preparation before the injection	16
2.2.1.1. Electrodes injection and fixing.....	16
2.2.1.2. Microfluidic platform sterilization	17
2.3. Human cardiac fibroblasts thawing procedure and culturing.....	17
2.4. Atrial and ventricular human cardiomyocytes thawing procedure	18
2.5. Atrial and ventricular human cardiomyocytes injection and culturing	18
2.6. Mechanical actuation of uStretch.....	19
2.7. Experimental plan for electrical and mechanical characterization	20
2.8. Video recording and MuscleMotion analysis	21
2.9. Statistical analysis.....	22
2.10. Field potential recording and WaveForms analysis.....	22
2.11. Immunostaining analysis.....	23
3 Results.....	25
3.1. Video recording and MuscleMotion analysis	25
3.1.1. Video recording and analysis results.....	25
3.2. Field potential recording and WaveForms analysis.....	30
3.2.1. Electrical results analysis	30

3.3. Immunostaining analysis 32

4 Discussion 34

5 Conclusion and future developments..... 36

6 Bibliography..... 39

List of Figures..... 49

List of Tables 53

List of symbols 55

Acknowledgments..... 57

1 Introduction

The heart is a hollow muscular organ, located near the anterior wall of the chest, just behind the breastbone, and its role is to collect deoxygenated blood from the body periphery and pump it back in the body before getting re-oxygenated by passing through the lungs [1]. The ability to generate force to push the blood through the cardiovascular system is up to the muscle which composes the heart itself. This muscle, from a macroscopic point of view, is an involuntary striated muscle composed by 30% of connective tissues and 70% of muscle fibres, which is called myocardium, surrounded externally by the pericardium and internally the endocardium. The pericardium is a thin mesodermal membrane composed by two layers, the fibrous pericardium, which is the outer layer, and the serous pericardium, which is the inner layer [1], [2]. This one is divided into three layers, one parietal layer, mostly composed by one layer of mesothelial cells and one of collagen, and two visceral layers. Between these two there is a cavity named as space or pericardial fluid. The endocardium is a thin translucent and whitish membrane that coats all the interior cavities and the valves. All these three components together form the heart wall. The heart can be divided into two sections, the left one and the right one [2]. Each section includes two cavities, an upper one called atrium and a lower one called ventricle. Between atria and ventricles there are 4 valves, the tricuspid valve, the pulmonary valve, the mitral valve and the aortic valve, able to regulate the bloodstream allowing the unidirectional flow avoiding the backflow [1].

Microscopically the heart is a highly organized complex tissues composed by different kind of cells. The main ones are:

- Cardiomyocytes: the main contractile cells of the heart, making up 30% of cardiac cells and are responsible for the heartbeat [3]. They present a striated appearance due to the interdigitated thin and thick filaments of actin and myosin. Surrounding them is the sarcolemma, a lipid membrane containing essential proteins for cell function.
- Fibroblasts: they comprise 30% of heart cells, play a role in collagen production, matrix remodelling and transduction of mechanical and electrical stimuli[3].
- Conduction cells: they include pacemaker cells and Purkinje cells, are involved in electrical signal transmission [2], [4].

- Cardiac stem cells: these cells possess the potential to differentiate into cardiomyocytes, endothelial cells, and smooth muscle cells for tissue regeneration [5].
- Endothelial cells: they cover blood vessels and heart chambers, regulating various functions such as thermoregulation, angiogenesis, and the exchange of molecules. They also play a role in supporting cardiomyocyte organization and function [6].

The mechanical and electrical contraction is made possible thanks to the presence of connections between cardiomyocytes. These occurs at the intercalated disks which contain adherens, desmosomal, and gap junctions. Adherens junctions link cells to the actin cytoskeleton, providing strength and allowing for uniform contraction of the heart, desmosomal junctions link cells to intermediate filaments offering structural support and gap junctions allow for the diffusion of molecules and propagation of electrical signals between cells [7], [8]. The rhythmic contractions of cardiac tissue are a result of its ability to generate and spread electrical impulses autonomously. These impulses start in the sinoatrial (SA) node, then move through the atrial walls to the atrioventricular (AV) node in a specific manner. The AV node slows down the impulse to allow the atria to fully contract before the signal is rapidly transmitted through the His bundle and Purkinje network to coordinate ventricle contractions. This ensures efficient blood pumping to both the lungs and body [7]. Action potentials originate from the SA nodal cells, also known as pacemaker cells, situated in the right atrium. The SA node produces spontaneous action potentials that travel through the atria and ventricles, causing the contraction of atrial and ventricular myocytes. Nodal cells, atrial cells, and ventricular cells have distinct morphological, molecular, and functional characteristics, resulting in differences in their electrophysiological and contractile properties [9]. Electrically the differences lie on the action potential which has five distinct phases:

- Phase 0: the membrane is rapidly depolarized from a resting hyperpolarized potential (approximately -80 mV or -85 mV in atrial or ventricular myocytes, respectively) to a positive potential (approximately +30 mV) [10]. When the atrial or ventricular myocytes are electrically stimulated, the initial membrane depolarization opens the fast-activating voltage-gated sodium channels;
- Phase 1: this phase is characterized by a transient partial repolarization which occurs when inward sodium current (I_{Na}) is rapidly inactivated and transient outward current (I_{to}) is activated [11]. Duration and shape of early phase 1 repolarization are thought to be modulated by I_{to} . Reducing I_{to} results in an extended action potential duration, leading to a stronger contraction force because of increased calcium influx through L-type calcium channels. Atrial myocytes have shorter and less intense action potentials compared to ventricular myocytes, in part due to the larger amplitude of atrial I_{to} [12];

- Phase 2: The distinct feature of the cardiac action potential is the presence of a depolarized plateau in phase 2 that lasts for a few hundred milliseconds. This plateau is the main difference between atrial and ventricular action potentials [12]. During phase 2, a delicate equilibrium is maintained between the inward L-type calcium current ($I_{Ca,L}$) and the outward delayed rectifier potassium current (I_K). The slower activation of $I_{Ca,L}$ compared to I_{Na} results in a prolonged inward current. However, this inward current diminishes due to calcium- and voltage-dependent inactivation while being counterbalanced by the outward I_K . In atrial myocytes, the strong ultrarapid delayed rectifier (I_{Kur}) dominates the outward current in phase 2, leading to a shorter phase 2 duration compared to ventricular myocytes. This is due to the presence of potassium channels with higher conductance and faster activation kinetics in atrial myocytes;
- Phase 3: As the inward $I_{Ca,L}$ decreases toward the end of phase 2, I_K (comprising I_{Ks} , I_{Kr} , and the inward rectifier current I_{K1}) becomes more prominent and leads to the repolarization of phase 3. As phase 3 nears its end, channels for I_{Ks} and I_{Kr} eventually shut down because of the hyperpolarized membrane potential. However, I_{K1} continues to maintain the steady resting membrane potential [9];
- Phase 4: in this phase the resting membrane potential of atrial and ventricular myocytes is depicted. Due to ventricular myocytes having a higher level of inward rectifier expression compared to atrial myocytes, they exhibit a slightly more negative resting membrane potential [10].

All these differences result in two different waveforms that characterize the atrium and ventricle electrical behaviour (Figure 1.1).

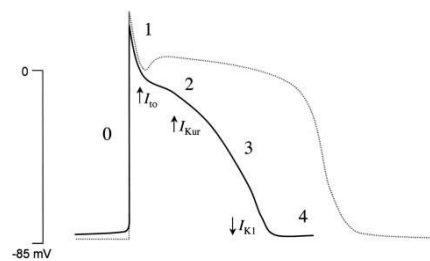


Figure 1.1: Comparison between ventricular action potential (dotted line) and atrial action potential (solid line). Ventricular action potential exhibits a less negative resting potential, a shortened plateau phase, and a slower terminal repolarization respect atrial one. Take from [13]

The contractile properties are different among atrial and ventricular cardiomyocytes because of the molecular composition. Myosin is the central molecular motor of the heart, which composes the cross-bridge cycling and regulates both ATP hydrolysis and mechanical production of contractile force. Myosin presents two heavy chains isoforms, α and β , and two light chains with two isoforms, MLC-2a specifics for atrial cardiomyocytes and MLC-2v for ventricular cardiomyocytes. Atrial myocardium is

recognized for its higher maximum shortening velocity (V_{max}) compared to ventricular myocardium [14]. The rate of active tension generation and relaxation in atrial myofibrils is also quicker than in ventricular myofibrils, which is thought to be due to differences in cross-bridge kinetics. Furthermore, the atrial working myocardium not only has a higher shortening rate but also produces less active tension compared to the ventricular myocardium. This difference in maximum tension development between the atrium and ventricle may be due to variations in the expression of myosin light chain (MLC) isoforms, which can influence aspects of cross-bridge cycling and force development [15].

Cardiovascular diseases (CVDs) are a major contributor to worldwide mortality, representing around 30% of all global deaths. These diseases are characterized by dysfunction in the vascular, cardiac, and nervous systems. There is currently a pressing demand for innovative medications and treatments to decrease the global impact of CVDs (Figure 1.2) [16].

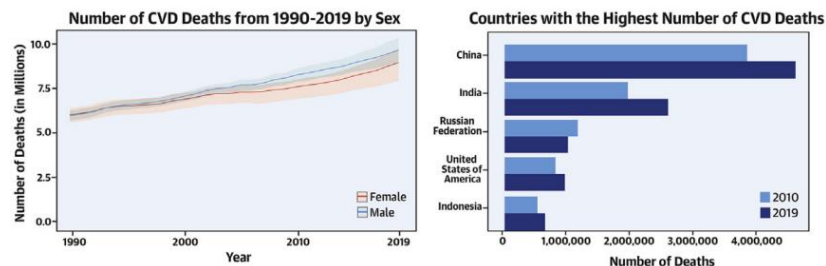


Figure 1.2: number of deaths through the years for CVD diseases. Adapted from [16]

Currently a lot of drugs are used for the CVD treatment, but these ones only slow down the pathogenic process. [16] This is the reason why transplantation continues to be the preferred method for treating heart disease, despite challenges such as donor shortages and the invasiveness of the surgery. Additionally, the process of drug development is costly and time-consuming before they can be brought to market. To improve the drug developmental process, drug screening testing is crucial and to solve ethical issues, in accordance with the 3Rs (Replacement, Reduction and Refinement), *in vitro* solutions are needed. In the last decade, promising *in vitro* techniques have been elaborated to mimic heart physiology, e.g. 2D cell culture and 3D monoculture. However, these models present a high throughput but on the other hand they are not physiologically relevant. To overcome this problem, heart on a chip model has emerged, offering an *in vitro* model able to recreate an *in vivo*-like environment useful to drug screening testing. In particular, the combination of 3D structured models with mechanical or electrical stimulation can enhance cell maturation, resulting in more consistent outcomes.

The utilization of heart-on-chip technology has shown great promise in replicating crucial features of cardiac tissue within a controlled laboratory environment, enabling researchers to stimulate the tissue in a precise manner for experimental investigations. This innovative technology is particularly valuable for emulating the functions of a

heart, facilitating drug testing and the study of specific diseases with a high level of accuracy.

By creating an *in vitro* model that closely mimics the behaviour of the heart, it is possible to effectively examine the effects of various drugs and develop potential treatments for diseases that affect cardiac function. To further enhance the fidelity of the cardiac model in terms of cellular development and maturity, a variety of advanced techniques are employed, including micropatterning of surfaces, the incorporation of supportive cells, the use of growth factors, hydrogels for creating a 3D environment, as well as mechanical and electrical stimulation. These sophisticated methods help to create a more realistic and functional model of cardiac tissue, enabling more accurate and informative research outcomes [17].

Madaline Campbell et al., developed a novel three-dimensional *in vitro* model of the heart which is a vascularized cardiac spheroid. This structure, which is composed by iPSC cardiomyocytes, cardiac fibroblasts and human coronary artery endothelial cells are co-cultured in hanging drop culture in ratios like those found in the human heart *in vivo*. The resulting 3D cellular structure has shown the potential to mimic the structure present in the heart. Moreover, this structure can also be used for studying cardiac physiology, disease and drug screening [18]. The major problem about the use of organoid remains the absence of vascular system which affects nutrient distribution within organoids impacting on their maturation and functionality [19].

Veldhuizen et al., created a cardiac tissue – on – chip with a 3D hydrogel to induce anisotropy in cardiac cells embedded in a 3D hydrogel and improve nutrient diffusion. They included a central patterned region using microposts to mimic the anisotropic structure of human tissue. Three different cell types were used to test the platform: neonatal ventricular rat-derived cardiomyocytes, human pluripotent stem cell-derived cardiomyocytes, and human cardiac fibroblasts (Figure 1.3). Their results showed that the microposts helped elongate and align the cells, creating a 3D anisotropic structure like that of the human heart but the main limitation of this kind of heart on a chip is the absence of an electrode guide for the electrical activity recording and stimulation[20].

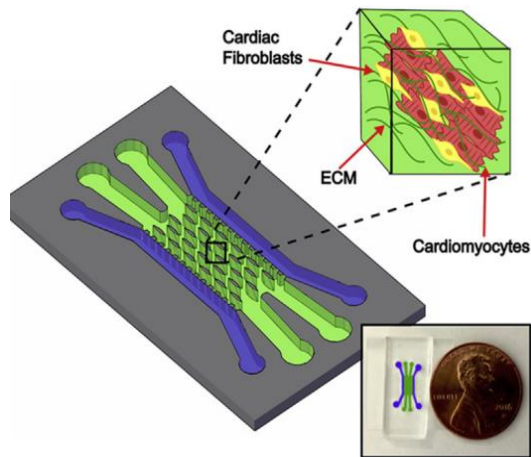


Figure 1.3: Schematic representation of the microfluidic device. The culture chamber is confined by trapezoidal micropillars, while the central part is patterned with an array of microposts that stimulate the cardiac tissue maturation. Adapted from [20]

In 2021, Zhang et al. introduced a heart-on-chip device equipped with microfluidic channels for extended culture, platinum wire electrodes to enhance the development of human induced pluripotent stem cell-derived cardiomyocytes (hiPSC-CMs) seeded on a gelatin thin layer through constant electrical stimulation, and gold electrode arrays for real-time recording of electrophysiological signals (Figure 1.4). This combined system offers a valuable means for evaluating drug effectiveness by observing the cells' capability to recover their normal beating rhythm post drug exposure [21]. The major limitation of this device remains in the number of layers and the fact that the last layer, which is a glass layer with four gold electrodes, is very fragile.

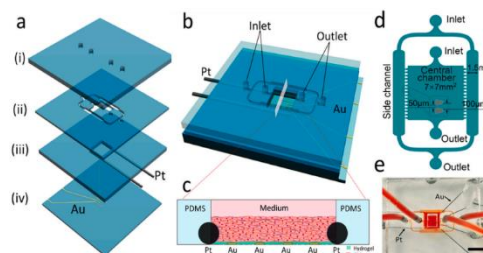


Figure 1.4: Platform made by three assembled PDMS layers bonded to a glass surface. (i) Top layer with four inlet/outlet holes, (ii) channel layer, (iii) layer with two parallel platinum (Pt) wire electrodes embedded at the bottom, (iv) bottom layer: glass plated with four gold electrodes (a). Three – dimensional schematic drawing (b). Cross – section of the device showing the distribution of cells within the device (c). Detailed design of the channel layer (ii) (d). Image of the assembled microfluidic device (e). Taken from [21]

For example, Marsano et al. created a heart-on-chip model to cultivate functional 3D cardiac microtissues using neonatal rat or human iPSC-CMs in a fibrin gel. They investigated the impact of physiological cyclic uniaxial strain on tissue maturity. To apply mechanical stimulation to the construct, a thin PDMS layer was placed below the cell culture chamber to create a pressure-actuated compartment. When positive pressure is applied, the flexible membrane moves up, causing controlled uniaxial strain in the microtissue. Releasing the pressure allows the PDMS membrane to return to its original position through elastic recoil. Through rhythmic pressure application, the model simulates systolic and diastolic phases. This method has shown to enhance mechanical and electrical connections between cells, promoting tissue maturation, resulting in synchronized beating and contractile properties (figure 1.5) [22].

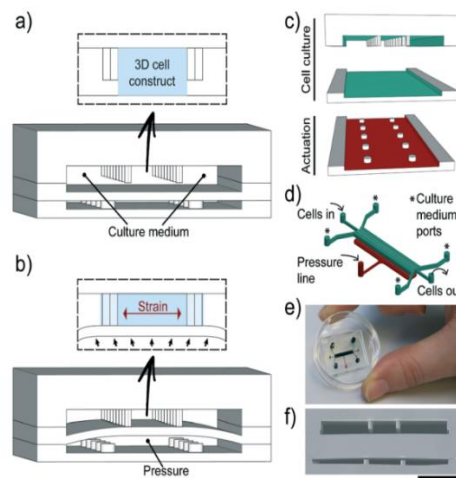


Figure 1.5: heart on a chip composed by two compartmentalized separated by a PDMS layer.

The central channel is filled with cell laden fibrin gel (a). The construct is repeatedly stimulated by exerting pressure on the lower compartment, causing the PDMS membrane to bend (b). The final device is achieved through the permanent bonding of three distinct PDMS layers (c). A 3D sketch of the microfluidic platform (d). Device photograph (e). Cross – sectional characterization of the device (f). Taken from [22]

For example, another platform has been implemented by Visone et al. to allow the application of the electrical stimulation using stainless steel electrodes placed parallelly to the construct in the media channels (figure 1.6)[23].

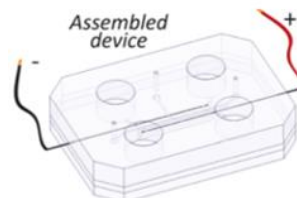


Figure 1.6: Electrical stimulation with two stainless steel electrodes inserted in parallel with the cell construct. Taken from [23]

In a successive study, R. Visone et al. designed a new heart on a chip device with a micro-electrode channel guide (μ ECG) used for field potential recording. The device is composed by three layers, the top layer, which contain the features of the chip, the actuation layer, which provides the mechanical stimulation simultaneously to the three microtissues, and the glass cover slide [24] (figure 1.7).

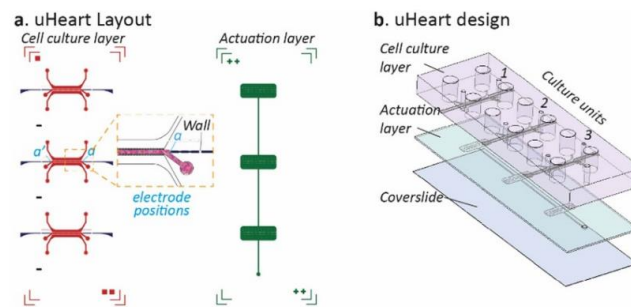


Figure 1.7: uHeart platform combining μ ECG technology with our existing beating heart on chip design. The uHeart platform is designed with a cell culture layer that includes three individual cell culture chambers (highlighted in red). Within each chamber, there is a 3D microtissue and two micro-guides for electrode insertions (highlighted in blue). The cell culture layer is intended to be connected to a single actuation layer (highlighted green) that delivers mechanical stimulation to all three microtissues at the same time (a). Inside the device, each cell culture chamber (1, 2, 3) is placed directly above its corresponding actuation chamber, which is sealed at the bottom with a cover slide for visual examination (b). Adapted from [24]

In all these models, one relevant limitation is sheared, i.e. that they allow the study of just one singular cardiac cell kind being a singular channel heart on a chip model. Being the heart a complex organ made by different kind of cell including atrial and ventricular cardiomyocytes, for this reason is necessary to introduce a new design able to allow the study simultaneously of both atrial and ventricular samples to fully mimic heart architecture. This research project, conducted in collaboration with BiomimX s.r.l., utilized a 3D heart on a chip model known as the uStretch platform to analyse the mechanical, electrical, and biological properties of atrial and ventricular microtissues. This innovative device addresses previous design constraints by being easy to produce, facilitating electrical recording, and allowing electrical stimulation. The initial phase involved analysing the mechanical behavior of atrial and ventricular samples to differentiate beating parameters under static and dynamic conditions. Video recordings were taken and analysed using the ImageJ tool MuscleMotion to compare parameters and identify variations among conditions. Subsequently, electrical characterization of the dynamic samples was performed to analyse important parameters such as beating period, field potential duration, and contraction amplitude using the WaveForms tool. The final step involved biological characterization through immunostaining to quantify protein expression levels specific to atrial and ventricular

samples, establishing a standard model for future drug screening tests. By creating a reliable benchmark for testing the effectiveness of new drugs in treating heart diseases, this research aims to propose a new chip design that enables the simultaneous culture of atrial and ventricular cardiomyocytes. By overcoming previous limitations, this innovative approach has the potential to greatly impact cardiac research and drug development.

2 Materials and methods

2.1. uHeart on chip

2.1.1. Microfluidic platform design

The chips used in this project to develop a full mature heart tissue are the uStretch® platform developed by BiomimX® S.r.l (Figure 2.1). The chip is made up of three layers, a Polydimethylsiloxane (PDMS) top layer, a PDMS actuation layer, and a glass coverslip. Each top layer contains three separate cell culture chambers, each with its own central channel surrounded by hanging pillars to support the 3D cell-laden fibrin gel. There are also two side medium channels for supplying their cell culture medium.



Figure 2.1: uStretch® platform produced by BiomimX® S.r.l

Each chamber has two holes, one at the beginning and one at the end of the central channel for injection inlet and outlet, each with a 1mm diameter. Additionally, there are four reservoirs in each chamber for medium replacement, connected to the side medium channels with a diameter of 5 mm each. The central channel dimensions are 300 μm width, 10 mm length, and 150 μm height and a 40 μm gap between the pillars. The actuation layer, with an 800 μm thickness, is shared by the three top layer chambers and consists of three interconnected rectangular compartments that can be pressurized and depressurized to stimulate mechanically the microtissues. It includes an inlet hole with a diameter of 1.5 mm for air entry. The chip design has two microelectrode channel guides for each side. The guide that allows the insertion of the electrode of recording into the culture channel is the recording guide, while the other that allows the insertion of the electrode of stimulation into the medium channel is the stimulation guide (Figure 2.2).

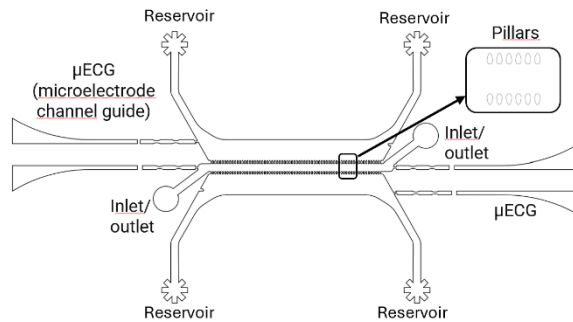


Figure 2.2 microfluidic one chamber CAD design of one top layer with a focus on the pillars shape.

When the actuation channel is pressurized, the membrane moves upwards causing a uniaxial deformation of the 3D microtissue (Figure 2.3). Upon pressure release, elastic recoil returns the membrane and construct to their original state. Mechanical stimulation is achieved with the help of uBoX (Figure 2.4), a portable control system that uses pressurized air and a graphical interface connected to a touch screen to adjust pressure patterns like duty cycle and stimulation frequency. In the "Heart" mode, uBoX applies a uniaxial strain of 10% at 1 Hz with a 50% duty cycle to mimic the systolic and diastolic phases of the heart.

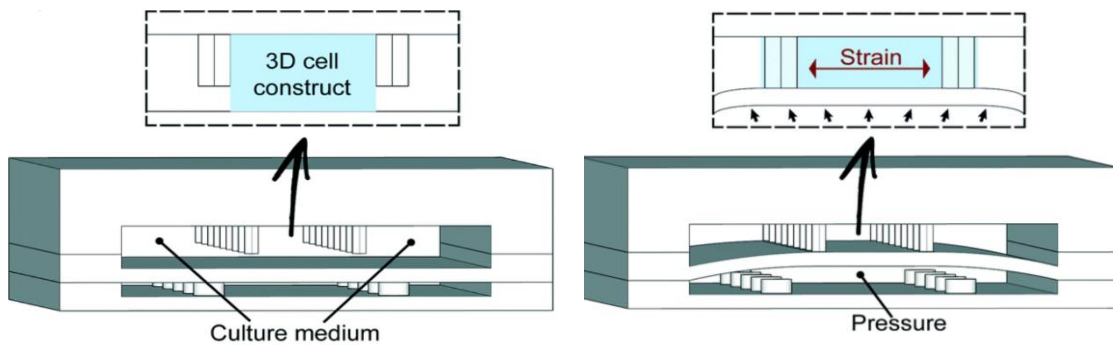


Figure 2.3: schematic representation of the uStretch cross-section in rest (picture on the right) and in actuation phase. Adapted from [22]



Figure 2.4: uBOX platform (BiomimX s.r.l.), which is a control system able to provide mechanical stimulation to each uStretch® platform.

2.1.2. Microfluidic device fabrication

The chips were produced at the beginning using techniques such as photolithography and soft lithography to obtain the master mold and at the end with replica molding using PDMS to obtain the final microfluidic device. The process began with master molds produced in a clean room at PoliFAB, Politecnico di Milano, using maskless photolithography. The negative photoresist (SU-8 MicroChem, USA) was applied using spin coating to control the final thickness, and then polymerized using direct laser writing (Heidelberg MLA100, Heidelberg Instruments) to create the desired features, which were the negative images of the final uStretch® products. Following exposure, uncrosslinked photoresist was removed with a developing solution (SU-8 developer; Microchem). The resulting product was a silicon wafer with the desired pattern, serving as the negative mold for the top layer made with PDMS. To prevent PDMS attachment, the wafer underwent surface treatment with tri-methyl-chloro-silane (Sigma-Aldrich) for 20 minutes. At this stage, a liquid PDMS (Sylgard® 184 Silicone elastomer kit, Farnell) was created by blending the two components (base elastomer and curing agent) in a 10:1 ratio by weight respectively. The resulting mixture was then degassed for 15 minutes in a vacuum chamber attached to a vacuum pump. The PDMS was subsequently poured onto a silicon wafer, degassed for another 15 minutes to eliminate any remaining bubbles, and then left to cure overnight on a level surface. The following day, the wafer was placed in an oven at 65°C for one hour, after which the PDMS stamps were peeled off and cut to create master molds. These master molds were then used to produce the epoxy resin molds. The epoxy resin mould was created to prevent the ongoing use of the fragile and costly micro-structured silicon wafer. To make this mould, the PDMS master mould was placed in a Petri dish with features facing up, ensuring no air bubbles were trapped. Component A and Component B of the resin (10 10 CSF, C-System) were mixed in a 2:1 ratio, degassed to remove bubbles, poured over the PDMS mould, and left to harden overnight on a flat

surface. The following day, the mold was taken off and the resin was left to be exposed to silane vapours for 15 minutes under the chemical hood. Removing all traces of silane was crucial due to its neurotoxic nature. To achieve this, a thin layer of PDMS was poured onto the resin, allowed to harden in the oven for approximately two hours, then peeled off and disposed of (Figure 2.5).

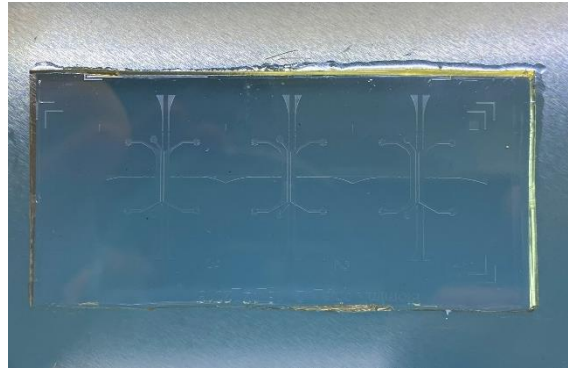


Figure 2.5: resin uStretch mold

For what concerns the actuation layer, this one is obtained pouring a thin layer of PDMS on the silicon wafer with the actuation features (Figure 2.6), with the same ratio of components previously said, to obtain 800 μ m thickness. Once the amount of PDMS is poured in the actuation silicon wafer, around 5g, and left in the vacuum chamber for at least 15 minutes to remove all the bubbles inside the PDMS. After this, the silicon wafer is left to solidify in the oven at 65°C for at least 2 hours.

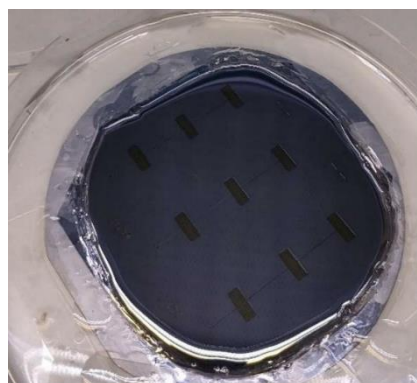


Figure 2.6: silicon actuation wafer already poured with PDMS

2.1.2.1. Microfluidic device assembling

Once top and actuation layer have been produced, they have to be aligned and bonded together. To do that the two surfaces to be attached of the two layers were exposed with an air plasma (Plasma Cleaner, Harrick Plasma, USA, model PDC-002). This treatment on the surface introduced hydroxyl groups, which enabled PDMS to form chemical bonds. The two layers were then aligned so that the central channel on the top layer, with the features facing the actuation layer, lined up with the rectangle on the actuation layer. The bonding process was made irreversible by heating the complex in an oven at 65°C for 20 minutes. Once bonded, the layers were removed from the silicon wafer, the actuation inlet was punched with a 1.5 mm biopsy punch, and the entire device was trimmed and reshaped with a Ted Pella blade to fit the dimensions of a glass coverslip (Menzel-Glaser 24 x 60 mm and 1.5 thickness) that supports the device. To complete the device, the chip and glass coverslip were subjected to plasma treatment again, bonded together, and then placed in the oven at 65°C for 24 hours to ensure the perfect adhesion.

2.1.2.2. Microfluidic device testing

Prior to utilizing the chips, a detailed microscopic inspection and pressure testing are conducted to ensure proper alignment of the punches and successful bonding. Following the initial microscopic examination, the chip is subjected to mechanical stimulation with air pressure twice the level used during experiments. The pressure

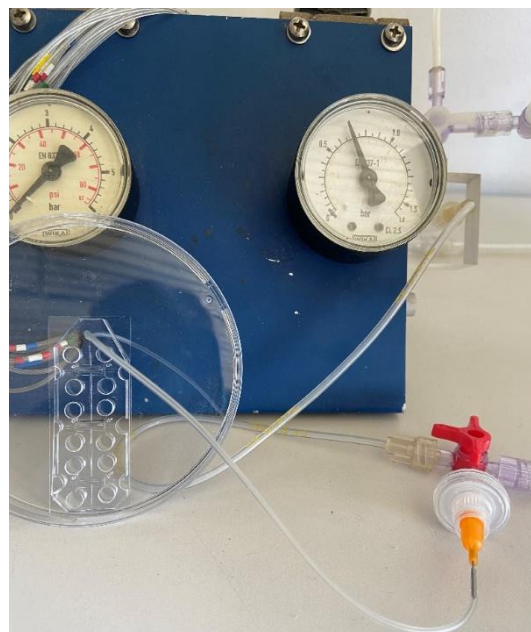


Figure 2.7: mechanical set up for uStretch testing with a 0.7 Bar pressure for at least 30 minutes.

level is maintained at 0.7 Bar for 30 minutes. If, after this procedure, the chips remain securely bonded and free of air bubbles between glass coverslip and actuation layers, they can proceed to integration with electrodes and sterilized (Figure 2.7).

2.1.2.3. Electrodes fabrication and testing

The process of electrode fabrication begins by assembling three key components: a gold pin, an electrical wire, and a 0.120mm needle. These components are carefully soldered together using an iron and tin soldering. Once the electrode is produced, it undergoes testing with a tester to ensure the soldering is secure and the continuity within it. Following successful testing, the electrode is prepared for the next stage of insertion into the chip through the μ ECG, enabling the recording of tissue electrical activity.

2.2. Device preparation before the injection

2.2.1.1. Electrodes injection and fixing

Electrodes insertion was performed inserting one of them through one of the μ ECG guides (Figure 2.8), specifically through the recording guide. After positioning at the channel entrance, the electrode was secured in place using a drop of PDMS with the predetermined component proportions. The assembly was then placed in the oven at 65°C for a minimum of 30 minute.

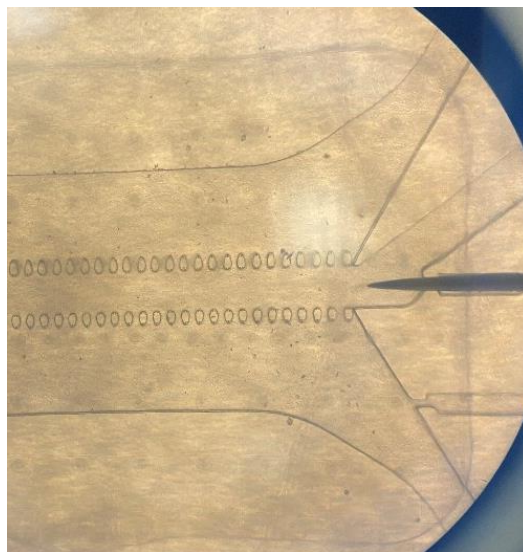


Figure 2.8: microscopic view of the electrode injection through μ ECG line

2.2.1.2. Microfluidic platform sterilization

Before the chip usage for biological experiments, they must be sterilized. Therefore, each chip was placed in suitable pouches, put into an autoclave, sterilized at 134°C, and then cooled to room temperature for at least 24 hours before the experiment. This procedure has no impact on the properties of PDMS.

2.3. Human cardiac fibroblasts thawing procedure and culturing

The process for thawing human cardiac fibroblasts provided by AXOL Bioscience involves several steps. Firstly, the cardiac fibroblasts medium has been prepared joining 40 ml of basal medium (fibroblast medium-2), 5% of fetal bovine serum (FBS), 1% of fibroblast growth supplement 2 (FGS-2) and 1% of penicillin/streptomycin solution (P/S solution). This medium is used exclusively for culturing the cells but not for the thawing. Afterwards, a T-75 flask is filled with 10 ml of complete cardiac fibroblast medium and put into the incubator for thirty minutes to have a medium temperature of 37°C and 5% of CO₂. The vial containing the cells is taken out from the liquid nitrogen (LN2), sprayed with 70% ethanol and opened and closed under the laminar flow (LAF) cabinet to release any pressure created by LN2 residuals and to avoid its explosion. The cryovial is defrosted inside the water bath, until a small crystalline is still present in the vial. The time required for the previous step is around 1/2 minutes. The cryovial is sprayed with 70% ethanol and put under the LAF cabinet. Once do that, the cryovial is opened and the suspension containing the cells plus the freezing mix is transferred into a 50 ml falcon tube containing 9 ml of complete medium. The complete medium used for the thawing is prepared with DMEM high glucose supplemented with 10% of FBS, 1% HEPES and 1% PSG. Once the cryovial is empty, this is washed with 1ml of complete medium. The falcon tube containing the cells is centrifuged a 220g for 5 minutes to separate the cells from the supernatant. The supernatant is removed and the cells are resuspended in 1 ml of cardiac fibroblasts medium. In the end the 1ml solution is transferred in the T-75 flask previously warmed up. For what concerns the culturing cardiac fibroblasts, the day after the thawing the medium is changed with fresh medium and after that the medium is changed every two days.

2.4. Atrial and ventricular human cardiomyocytes thawing procedure

The process for thawing human atrial and ventricular cardiomyocytes provided by AXOL Bioscience involves several steps. In the first place the thawing medium, called plating medium, is prepared. The plating medium, which is used exclusively for the cardiomyocytes thawing, is prepared cardio maintenance basal medium plus supplements, 10% of FBS, 1% of P/S solution and 0.1% of rock inhibitor. Once prepared, the medium is warmed up to 37°C. The two cryovials containing atrial and ventricular cardiomyocytes are taken from the LN2, sprayed with 70% ethanol and opened and closed under the LFA cabinet for the same reason as cardiac fibroblasts thawing procedure. Afterwards, the two cryovials are defrosted in the water bath until a small crystalline is still present in the vials. The 1ml solution contained in both cryovials is transferred into two 50ml falcon tube, one for atrial and one for ventricular cardiomyocytes. Each cryovial is washed with 1ml of plating medium and this is added at the 50ml falcon tube dropwise. The time requested for this step is 1 minute. Afterwards, 8 ml of plating medium is added for each falcon tube dropwise and this step requires the same amount of time of the previous one. These last two steps are performed that way to reduce the osmotic shock and to preserve the cellular viability. The two 50ml falcon tube are centrifuged at 200g for 5 minutes to separate the cells from the supernatant and this one is subsequently removed. For each falcon tube is added 1 ml of plating medium to resuspend the cells.

2.5. Atrial and ventricular human cardiomyocytes injection and culturing

Once the atrial, ventricular cardiomyocytes and cardiac fibroblasts thawing procedures have been performed and the three cellular kinds are resuspended in 1ml of their specific medium, the cells must be counted. This because the cardiac microtissues, both atrial and ventricular, are composed by 75% of cardiomyocytes and 25% of cardiac fibroblasts, moreover the final cell density must be in the range between 85×10^6 - 125×10^6 cells/ml in a final fibrin gel composed by 10 mg/ml of fibrinogen and 2.5 U/ml of thrombin. Firstly, a bucket with ice is sprayed with 70% ethanol and placed inside the LFA cabinet, secondly prepare the two components for the fibrin gel. Starting from a stock solution of 100mg/ml of fibrinogen and 100U/ml of thrombin, the first one has to be diluted with phosphate buffered saline (PBS) to have a final concentration of 50mg/ml and the second one has to be diluted with maintenance medium to have a final concentration of 6.25U/ml. After determining the right amount of cardiac fibroblasts to be mixed with atrial and ventricular cardiomyocytes, the total

solution (atrial or ventricular cardiomyocytes plus cardiofibroblasts) is divided into 2 eppendorf in order to have a final concentration per eppendorf of 85×10^6 - 125×10^6 cells/ml. once do that, the eppendorf are centrifuged at 200g for 5 minutes. Afterwards the supernatant is removed and the pellet, which is approximately 4 μ l, is mixed with 4 μ l of the diluted thrombin and 2 μ l of diluted fibrinogen to create cell-laden fibrin gel. Mixing 3 times with a 10 μ l pipette the total solution, the injection is performed. The total 10 μ l solution is enough to perform at least 5 injections. After the injection, the chips with a drop of PBS, are put in the incubator for 8 minutes to let the gel cross-link. Once the gel is crosslink, for the injection day (day 0), with plating medium plus ACA(2mg/ml), the channels are hydrated and the medium is used for the first day of culturing.

2.6. Mechanical actuation of uStretch

The process of preparing the uStretch mechanical actuation system is crucial for ensuring its proper functionality. As outlined in the procedure, the initial step involves removing any air from the actuation chambers by injecting PBS into the tygon tube until a drop emerges. This is followed by carefully inserting one end of the tygon tube into the actuation hole of the uStretch and injecting the PBS into the chips to confirm correct insertion. Subsequently, the syringe is disconnected and a 0.22 μ m sterile filter is attached before connecting the system to air at 0.35 bar to fill the actuation of the uStretch for a minimum of 45 minutes. During this time, thorough checks are conducted on all actuation chambers and medium channels to ensure optimal functionality, with any remaining bubbles obstructing the medium flow being promptly removed by rehydrating the blocked channels. For the daily maintenance of the system, a cardio maintenance medium with 10% of PS and ACA 100% is used, with the ACA concentration gradually decreasing with each subsequent medium change. This meticulous approach to preparing and maintaining the uStretch mechanical actuation system helps to ensure consistent and reliable performance for experimental purposes. The medium change has to be done every day decreasing the ACA concentration each time following this pattern:

- Day 0, 1: 100% ACA (i.e. 2mg/ml);
- Day2: 80% ACA;
- Day3: 70% ACA;
- Day4: 60% ACA ;

- Day5-on: 50% AC.

For the first experiment, has been decided to verify the mechanical stimulation effect on the beating microtissues. Thus, for each condition, atrial and ventricular microtissues, has been taken one uStretch as static, without stimulation, to make comparisons.

2.7. Experimental plan for electrical and mechanical characterization

The protocol has been followed of the mechanical characterization, which aims to understand the mechanical stimulation effect on the atrial and ventricular microtissues behaviour, started from day 0, the injection day, continuing from the day 1, the actuation day, when it's been applied the mechanical stimulation with a 0.35 Bar, with 1Hz frequency and a 50% duty cycle, to day 11. Moreover, from day 5 to day 11 have been performed the video recording and analysis (Figure 2.9). For this experiment have been used some chips as static, as a control condition, and some chips as dynamic.

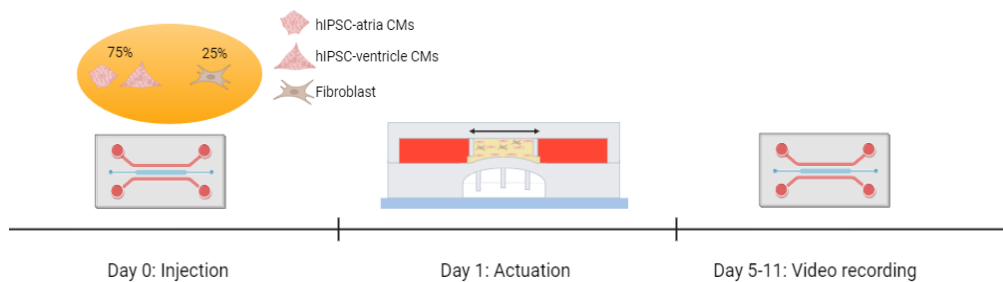


Figure 2.9: protocol followed for the mechanical characterization analysis and video recording

During the electrical characterization, the process remained consistent, with the exception of the final days where video recording was omitted and field potential was instead recorded (Figure 2.10). In this experiment, only ventricular samples were collected instead of both static and dynamic samples.

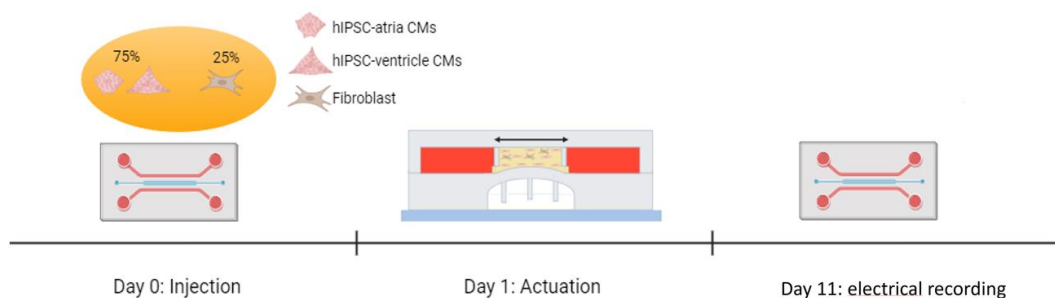


Figure 2.10: protocol followed for the electrical characterization analysis and video recording

2.8. Video recording and MuscleMotion analysis

Video recording was performed using a microscope with a 10X magnification for a video length of 60 seconds, at a rate of 20 frames per second. The analysis of the video recording was conducted with MuscleMotion, an ImageJ® plugin designed for use with standard laboratory and clinical imaging equipment, allowing for quantitative analysis of beating cardiac microtissues [25]. This program can analyse the kinetics of beating microtissues and extract relevant parameters. The tool, which requests the recorded video frame per second to be set, processes one video as input and generates 7 files as output, including the contraction trend over time and comprehensive results containing the four key parameters of interest: contraction amplitude, time to peak, relaxation time, and beating period. These parameters are determined based on pixel variations between a reference frame and the current frame. For each microtissue have been taken two videos, one about the central portion and one for the best lateral portion, and only the best was taken as measurement candidate. This video recording has been made for all the microtissues for the days 5, 6, 7, 8 and 11 of culturing. Afterwards, each video of each day has been divided into three Regions (Figure 2.11) of Interest (ROIs) and each one was individually analysed by MuscleMotion to calculate the parameters of interest. The results from the three ROIs of one microtissue were then averaged.

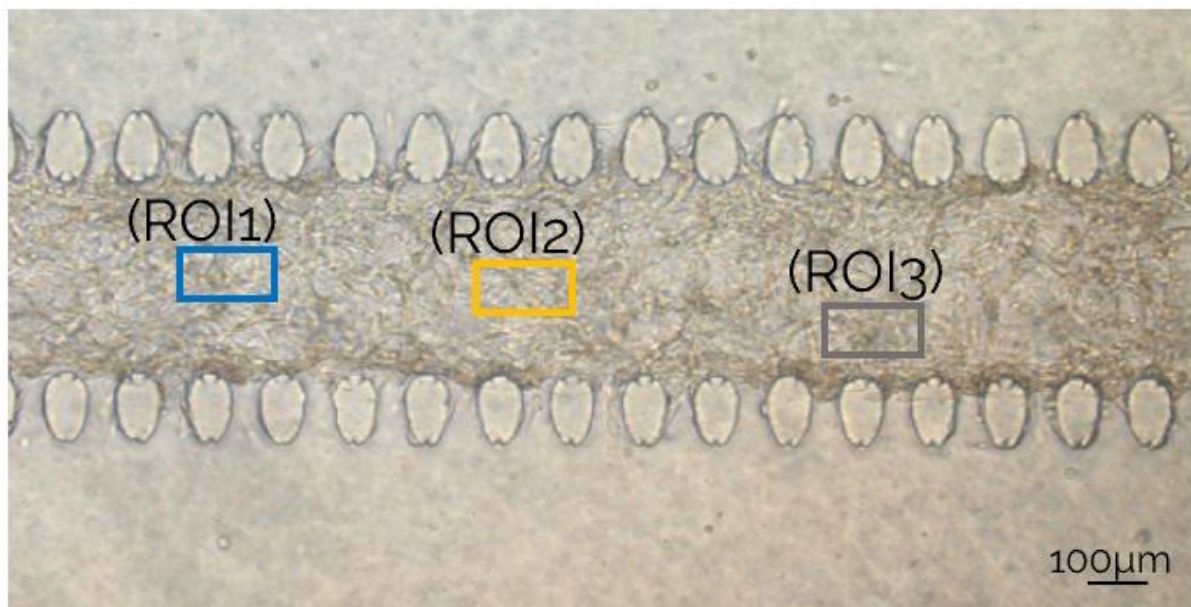


Figure 2.11: three ROIs taken from one microtissue for MuscleMotion analysis

Moreover, to verify the mechanical stimulation effect on the microtissues pulse, it has been calculated the Pearson's correlation coefficient. This parameter has been calculated between the normalized data about the contraction trend over time file to verify and quantify the synchronous beating of the construct seeing if there were any differences between the dynamic and static microtissues. All this data have been analysed and compared through the days in order to see the specific day which was the best candidate in terms of Pearson's correlation coefficient, contraction amplitude, beating period and relaxation time.

2.9. Statistical analysis

The average values for beating period, Person's correlation coefficient, contraction amplitude, time to peak, and time to relaxation were calculated for each sample of static and dynamic atrial and ventricular microtissues. The data was then separated based on static and dynamic conditions to analyse how mechanical stimulation influenced cell development and beating characteristics. Statistical analyses were performed using GraphPad Prism 9 software. Normal distribution of datasets was assessed using One Way Anova with Tukey's multiple comparison for comparisons across all days between the data. Significance levels were set as * $p < 0.05$, ** $p < 0.01$, *** $p < 0.001$, and **** $p < 0.0001$ and the results were presented as mean \pm SD

2.10. Field potential recording and WaveForms analysis

To understand the electrical behaviour difference between atrial and ventricular microtissues, the field potential has been recorded at day 11. Doing that, for each signal, has been derived three main parameters, the spike amplitude, beating period, which is the time between two depolarization peaks, and field potential duration, which is the time between the depolarization peak and repolarization peak (Figure 2.12).

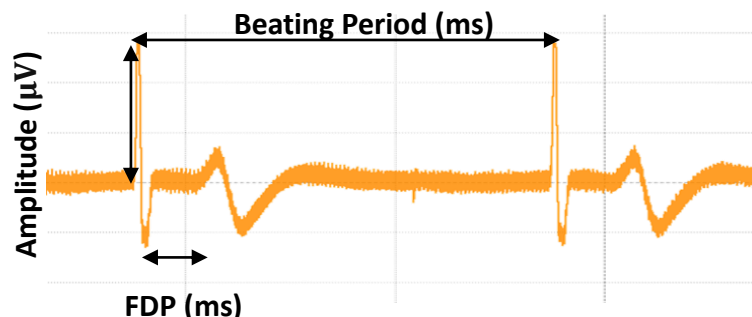


Figure 2.12: recorded ECG signal showing the three parameters of interest, which are the beating period, spike amplitude and field potential duration

The acquisition system used is composed by 5 main components, recording electrode, reference electrode (AgCl ground electrode), pre-amplifier, extracellular amplifier and electronic board (Digilent). The recording electrodes, which consists of stainless-steel microneedle, was carefully injected inside the μ Stretch through the μ ECG line [26]. An AgCl ground electrode was placed in one of the two reservoirs containing cell culture medium in the opposite side respect to the recording electrode (figure 2.13). Prior to each measurement, the cell culture medium was refreshed at least 1 hour in advance. The uStretch was maintained in an incubator at 37°C with 5% CO₂ during the testing period, while the electrodes were connected to an extracellular amplifier (Ext-02b, Npi Electronic GmbH, Germany) with a gain of 1×10^4 and a bandpass filter ranging from 0.3 Hz to 10 kHz. The field potentials of both atrial and ventricular microtissues were captured using an electronic board (Analog Discovery 2, Digilent, Washington) at a sampling rate of 2000 samples per second.

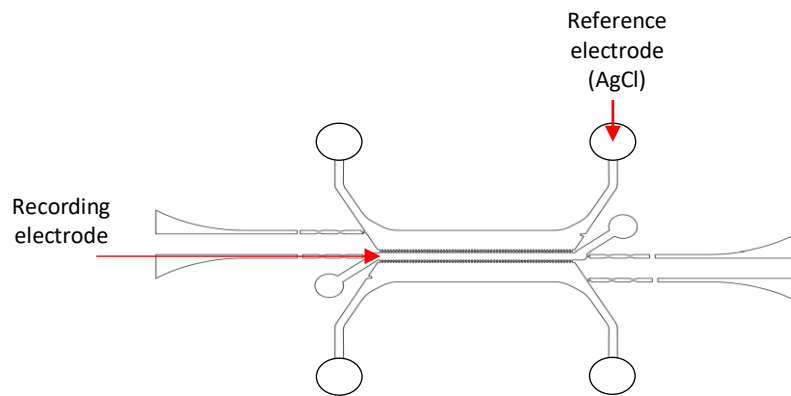


Figure 2.13: schematic representation about the electric set-up acquisition system.

2.11. Immunostaining analysis

Immunofluorescence analysis was performed at the end of the electrical recording experiment. To start, microdevices were fixated following a specific fixation procedure. The used medium was taken out from the wells and the medium chambers were cleansed with PBS two times, with a gap within about 2 minutes, using filling two reservoirs per time to completely wash the channel. In a chemical hood, the PBS was removed and warm paraformaldehyde (PFA) 4% (Merck, 158127) was introduced (~200 μ L) on one side, allowing it to reach the other side of the microtissue. The PFA rinsing was repeated and the device was left at room temperature for 20 minutes with PFA remaining inside for fixation. Subsequently, the PFA was taken out and PBS was added to the wells for a final wash following the procedure previously said.

Afterwards, for a proper conservation, the chip has been placed upside down in a Petri dish and covered with PBS. The Petri dish has been sealed with parafilm and put into the fridge at 4°C until the immunostaining day.

After conducting literature research, the decision was made to assess the levels of certain cardiac-related markers. To evaluate structural organization of the atrial and ventricular microtissues have been selected the cardiac troponin I (rabbit, IgG2a, SantaCruz, 1:100), which assess the cardiac phenotype and maturation, the vimentin(chicken, IgY, Abcam 1:1000), which stains the cardiac fibroblasts, DAPI for the nuclei staining (1:100), the myosin light chain-2 ventricular (rabbit, IgG, Abcam, 1:150), which is a protein obtained after the myosin differentiation and is specific for ventricular cardiomyocytes, and the sarcolipin (rabbit, IgG, Thermofisher, 1:100), which is a specific protein of atrial cardiomyocytes. The sample for immunofluorescence was washed twice with PBS, with a minimum of 10 minutes allotted for each wash. A blocking and permeabilizing solution, containing 0.1% Tween-20 (Sigma Aldrich, 038K00914), 2% BSA (w/v), and PBS, was added to the wells in 150 µl increments. This solution was then allowed to incubate at room temperature for 1 hour. The presence of Tween-20 serves to permeabilize the cell membrane, enabling the staining of cytoskeletal proteins, while BSA works to prevent non-specific binding. After that, the blocking solution was removed and 200µl primary antibody solution, with the specific dilution for each antibody, per microtissues, which is formed by primary antibody and 0.5% Goat serum (Sigma Aldrich, SLCK7210), was added in the 4 wells. The microtissues were left overnight at 4°C in the fridge. The primary antibody solution was subsequently aspirated from the wells, and the microconstructs were then washed twice with PBS, with a 20-minute incubation period between each wash. The secondary antibodies used were Alexa Fluor 488 Goat anti-mouse (Invitrogen, A-11008), Alexa Fluor 488 Goat anti-chicken (Invitrogen, A-11008), Alexa Fluor 546 goat anti-mouse (Invitrogen, A-11030) and Alexa Fluor 546 goat anti-rabbit (Invitrogen, A-11030). The samples were incubated at room temperature on a rocker for 2 hours with the secondary antibody solution. This solution was removed and replaced with a final working solution of 300 nM 4',6-diamidino-2-phenylindole (DAPI) diluted in PBS (Invitrogen, D1306). This solution was injected into the devices (200 µl for each construct) and incubated in the dark (covered with aluminium foil) overnight at 4°C to stain cell nuclei for identification.

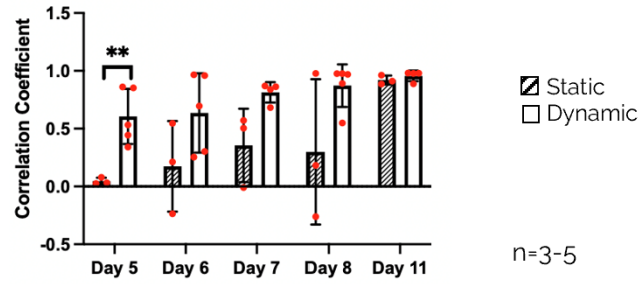
3 Results

3.1. Video recording and MuscleMotion analysis

3.1.1. Video recording and analysis results

The videos captured on days 5, day 6, day 7, day 8 and day 11 of the culturing process were examined to assess the impact of mechanical stimulation on atrial and ventricular microtissues. A comparison of the two types of microtissues was conducted to better understand their differences in behaviour. Thus, these videos, as previously said, were analysed with MuscleMotion and all the results obtained are represented with histograms with their mean values and standard deviations. The initial comparison is between static and dynamic conditions for both atrial and ventricular samples to better understand the mechanical stimulation effect. The Pearson's correlation coefficient has been utilized to compare them. The data from the graphs show a significant difference in the Pearson's correlation coefficient, especially on the initial day of measurement (day 5). For atrial samples in day 5, the mean for the static condition is 0.0451847667 with a standard deviation of ± 0.029757 , while the dynamic condition has a mean of 0.6062896478 and a standard deviation of ± 0.238296 . Ventricular samples in day 5 also show a similar trend, with a mean of 0.270748 and a standard deviation of ± 0.069574 for the static condition, and a mean of 0.9435566 and a standard deviation of ± 0.058113 for the dynamic condition. The dynamic samples consistently exhibit a higher Pearson's correlation coefficient compared to the static samples, although this disparity lessens through the days (Figure 3.1).

Atrial microtissues



Ventricular microtissues

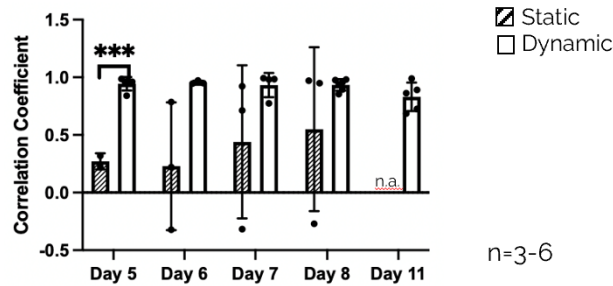


Figure 3.1: comparison between dynamic and static condition for both atrial (red dots) and ventricular (black dots) microtissues. Statistical test performed to obtain statistical significance (** $P < 0.01$ and *** $P < 0.001$).

A comparison of dynamic samples reveals that ventricular microtissues exhibit more synchronized beating than atrial microtissues on most days, except for the final day of measurement, which is day 11, where ventricular samples have a 0.83 ± 0.1238 Pearson's correlation coefficient and atrial samples have a 0.9563 ± 0.04641 Pearson's correlation coefficient. This trend is further supported by an examination of static conditions, although the high standard deviation in this analysis renders the results statistically insignificant (figure 3.2).

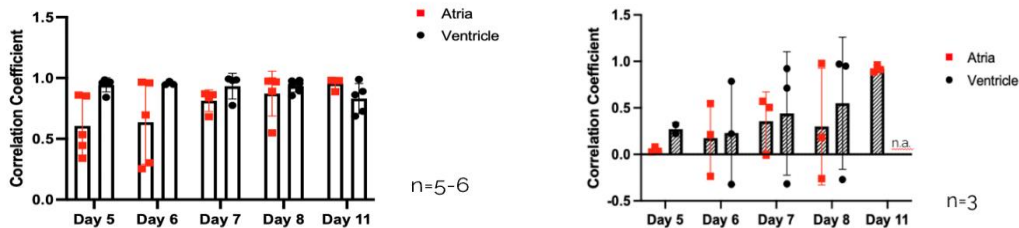


Figure 3.2: on the left histogram there is the correlation coefficient comparison between dynamic samples and on the right histogram between static ones.

Afterwards, once understood the mechanical stimulation effort, all other MuscleMotion parameters have been analysed singularly (Figure 3.3) for each condition and subsequently compared (Figure 3.4).

Regarding atrial dynamic microtissues, the beating period remains consistent over the days, starting from an overall mean of 2176.76 ms with a standard deviation of ± 506.557 ms on day 5, and decreasing to an overall mean of 2066.941 ms with a standard deviation of ± 556.7486 ms. The contraction amplitude increases over time, with a starting value of 35.17427 a.u. ± 12.44349 on day 5, peaking at 149.9467 a.u. ± 40.63089 on day 8. The time to peak slightly decreases from an overall mean of 694.5876 ms ± 508.9706 ms on day 5 to 532.8836 ms ± 155.1602 ms on day 11. Similarly, the relaxation time slightly increases from an overall mean of 651.2254 ms ± 289.2517 ms on day 5 to 795.436 ms ± 129.0878 ms on day 11. In contrast, for ventricular microtissues, the beating period slightly decreases over the days, starting from an overall mean of 2475.125 ms with a standard deviation of ± 717.9613 ms on day 5, to 1510.365 ms with a standard deviation of ± 453.87 ms. The contraction amplitude increases over time, starting at 37.30596 a.u. ± 19.89733 on day 5 and peaking at 82.62861 a.u. ± 11.29409 on day 7. The time to peak slightly decreases from an overall mean of 645.7756 ms ± 111.4107 ms on day 5 to 585.6717 ms ± 264.0015 ms on day 11. The time to relaxation also slightly decreases from an overall mean of 623.3852 ms ± 188.8935 ms on day 5 to 465.8487 ms ± 145.6313 ms on day 11.

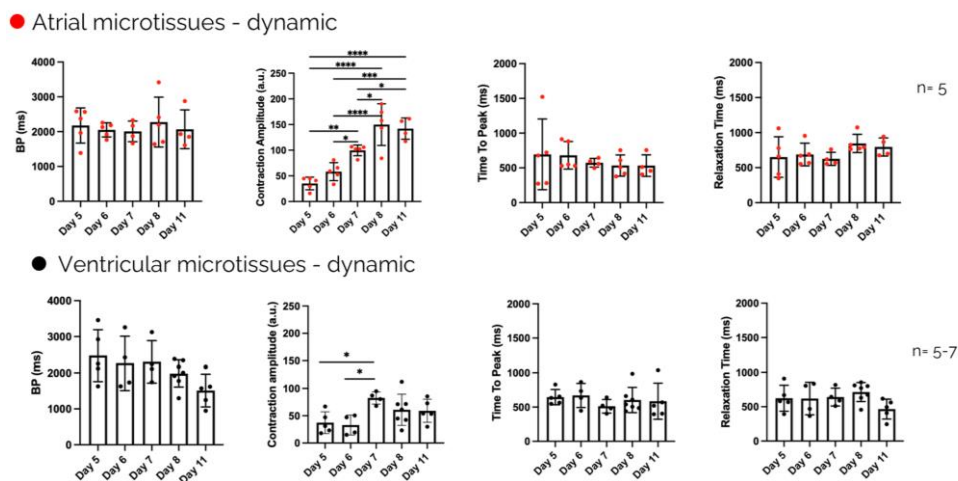


Figure 3.3: graphs showing beating period, contraction amplitude, time to peak and relaxation time for atrial dynamic microtissues (red dots), from day 5 to day 11 of culturing, and ventricular dynamic microtissues (black dots). Statistical test performed to obtain statistical significance (**** $P < 0.0001$, *** $P < 0.001$, ** $P < 0.01$ and * $P < 0.05$).

In comparing the data from atrial and ventricular dynamic samples, there are differences between the two conditions (Figure 3.4). The beating period initially shows slightly higher values in atrial samples for the first three days, but this trend reverses in the final two days. Similarly, the contraction amplitude in atrial samples is slightly higher in the first three days, but this difference becomes statistically significant in the last two days. Atrial samples have an amplitude of 149.94 ± 40.63 a.u. at day 8 and 142.055 ± 20.65 a.u. at day 11, in the meantime ventricular samples have an amplitude of 56.81 ± 33.80 at day 8 and 59.15 ± 21.17 at day 11. On the other hand, the time to peak shows no significant difference between the two sample types and remains relatively constant over the 5-day period. The relaxation time also shows a minor difference in the first three days, with atrial samples exhibiting longer relaxation times, which becomes more pronounced in the last two days.

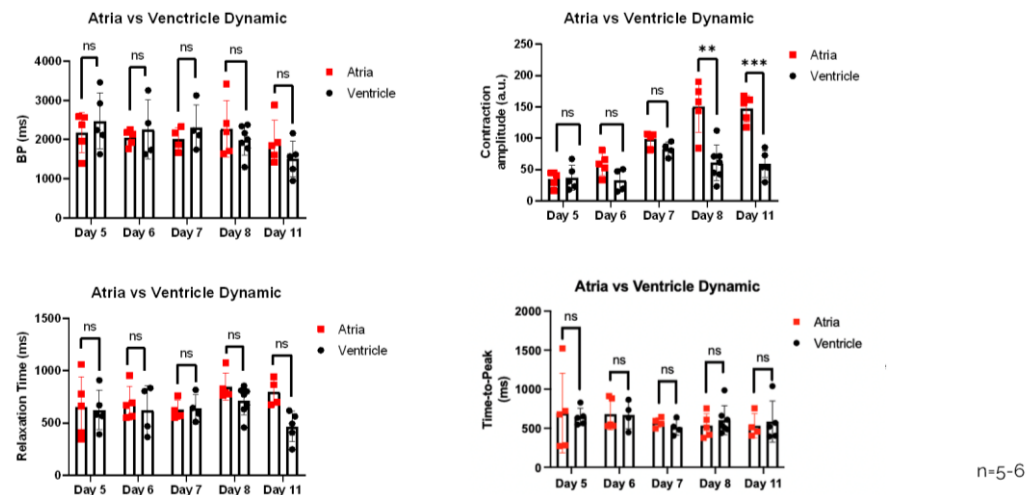
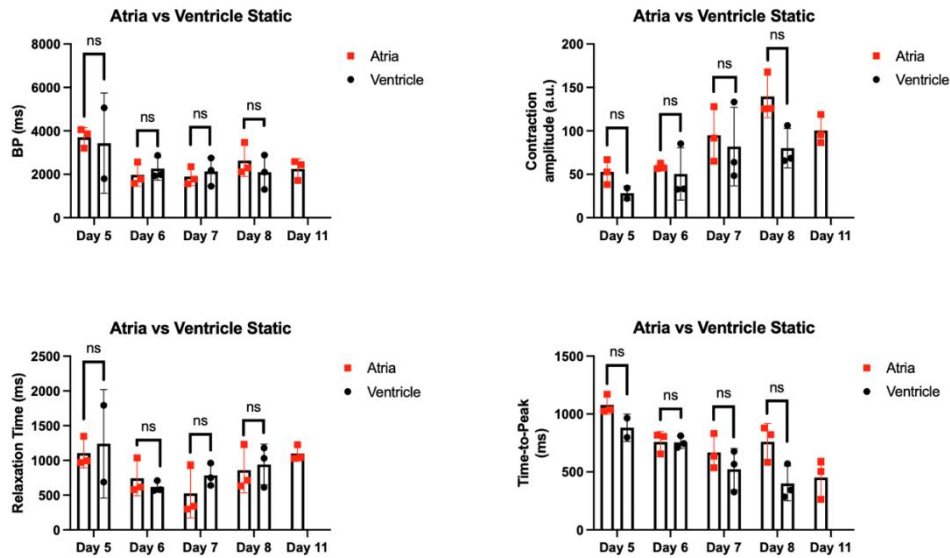


Figure 3.4 graphs showing comparisons between atrial and ventricular dynamic microtissues for beating period, contraction amplitude, relaxation time and time to peak through the days of culturing. Statistical test performed to obtain statistical significance (** $P < 0.01$, *** $P < 0.001$ and not significant (ns) with a $P > 0.05$).

Comparing the static data samples, although not statistically significant, these graphs reconfirm the data of the dynamic condition. In fact, this happens expect for one parameter, the relaxation time where the ventricles are higher than atrial ones (Figure 3.5).



n=3-6

Figure 3.5: graphs showing comparisons between atrial and ventricular static microtissues for beating period, contraction amplitude, relaxation time and time to peak through the days of culturing. Statistical test performed to obtain statistical significance (ns with $P > 0.05$).

3.2. Field potential recording and WaveForms analysis

3.2.1. Electrical results analysis

The analysis of four field potential parameters for the atrium and ventricle revealed distinct differences in their behavior. The analysis showed that atrial samples, indicated by red dots, had an average spike amplitude of 293.33 μV with a small standard deviation of $\pm 9.8657 \mu\text{V}$, while ventricular samples, represented by black dots, had a lower average spike amplitude of 154.25 μV with a wider standard deviation of $\pm 92.13 \mu\text{V}$ (Figure 3.6).

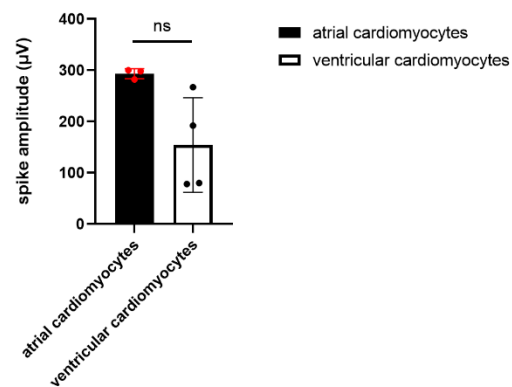


Figure 3.6: spike amplitude comparison between atrial and ventricular samples at day 11 of culturing. Statistical test performed to obtain statistical significance (*ns* with $P>0.05$).

In terms of the other three parameters, atrial cardiomyocytes have a mean beating period of 1074.667 ms \pm 42.194 ms, while ventricular cardiomyocytes have a mean beating period of 1120 ms \pm 668.691 ms. The field potential duration (FDP) is 216.333 ms \pm 46.45 ms for atrial samples and 309.75 ms \pm 81.79 ms for ventricular samples. When using Fridericia's correction, the FDP is 212.33 ms \pm 44.07 ms for atrial samples and 305 ms \pm 55.19 ms for ventricular samples (Figure 3.7).

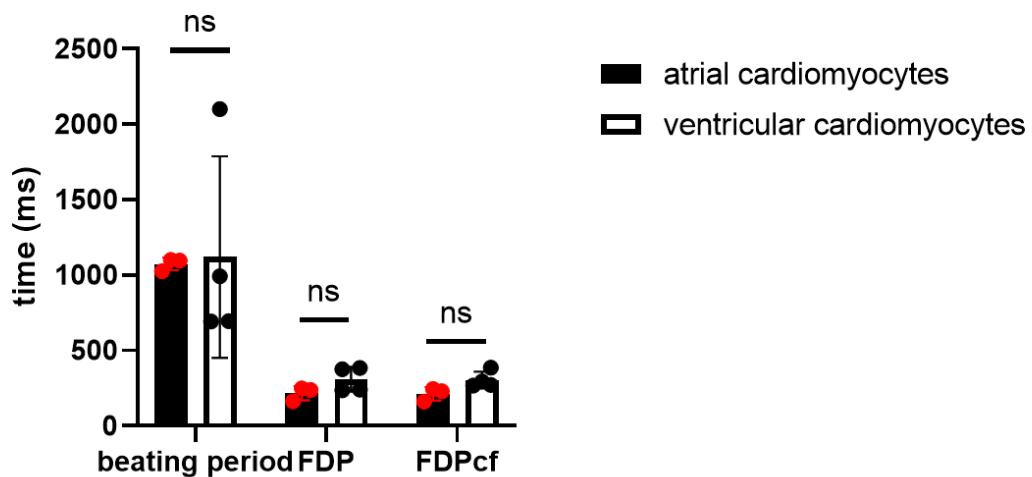


Figure 3.7: beating period, field potential duration and field potential duration after Fridericia's correction comparison between atrial and ventricular samples after 11 day of culturing. Statistical test performed to obtain statistical significance (ns with $P > 0.05$).

These results suggest that there are distinct differences in the electrical activity between atrial and ventricular cardiomyocytes, with atrial samples demonstrating higher spike amplitudes, shorter beating periods, and shorter field potential durations compared to ventricular samples. Moreover, the standard deviations for both parameters are also generally lower for atrial samples compared to ventricular samples. This indicate that atrial cardiomyocytes have more consistent electrical activity compared to ventricular cardiomyocytes.

3.3. Immunostaining analysis

For the biological characterization, literature research was conducted to identify specific markers for both atrial and ventricular dynamic samples utilized in immunostaining studies. After 11 days of culturing the samples were fixed and the immunostaining was performed. Atrial and ventricular samples were stained with cardiac troponin I (cTn1), ventricular myosin light chain-2 (MLC2v), sarcolipin (SLN) and vimentin (VTN) [27]. Ventricular samples have highly expressed cardiac troponin I, vimentin and ventricular myosin light chain-2, which was expected being a ventricular specific marker [27] (Figure 3.8). On the other hand, they haven't expressed sarcolipin, which was expected being an atrial specific marker. Atrial samples have highly expressed vimentin, cardiac troponin I and sarcolipin (Figure 3.9), which was expected being an atrial specific marker [27]. Comparing atrial against ventricular samples, ventricular samples show a higher expression of cardiac troponin I than ventricular ones. On the other hand, ventricular microtissues show a higher expression of vimentin (Figure 3.10).

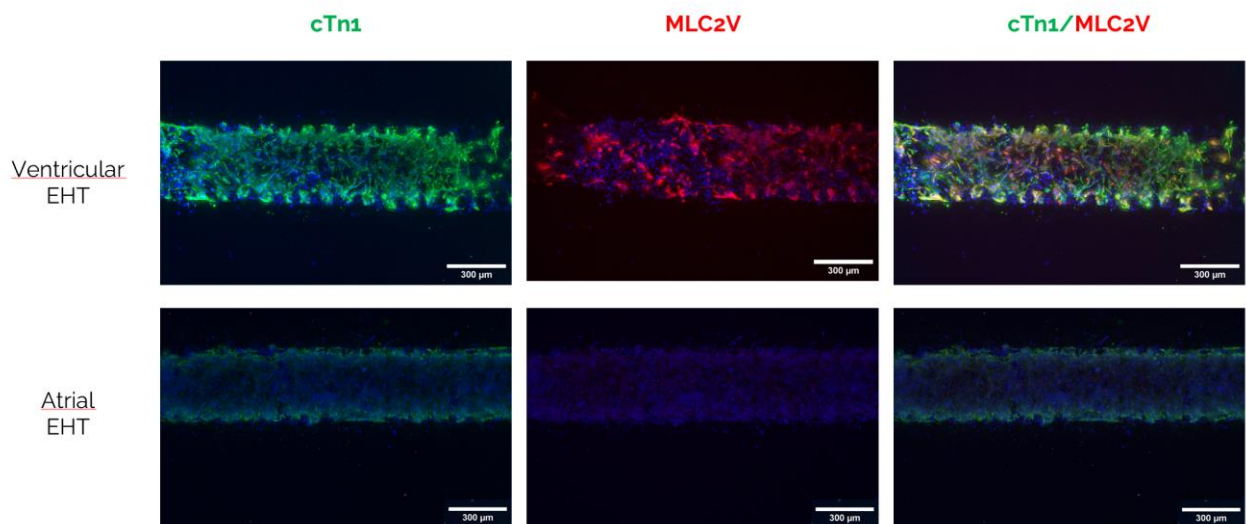


Figure 3.8: representative images of atrial (last three images) and ventricular (first three images) microtissues after 11 days of culturing in 3D in gel fibrin. Cardiac fibroblasts are identified by cardiac troponin I (green), ventricular cardiomyocytes by ventricular myosin light chain 2 (red) and atrial cardiomyocytes are not stained because they don't express myosin light chain ventricular being a specific ventricular marker. Nuclei are stained with DAPI (blue).

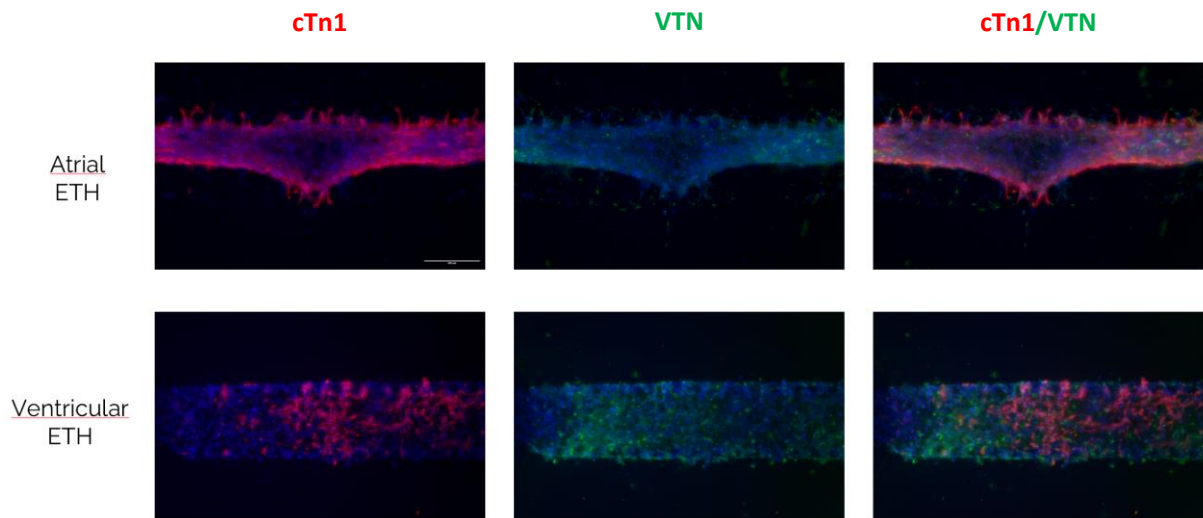


Figure 3.9 : representative images of atrial (last three images) and ventricular (first three images) microtissues after 11 days of culturing in 3D in gel fibrin. Cardiac fibroblasts are identified by cardiac troponin I (green), atrial cardiomyocytes by sarcolipin (red) and ventricular cardiomyocytes are not stained because they don't express sarcolipin being a specific atrial marker. Nuclei are stained with DAPI (blue).

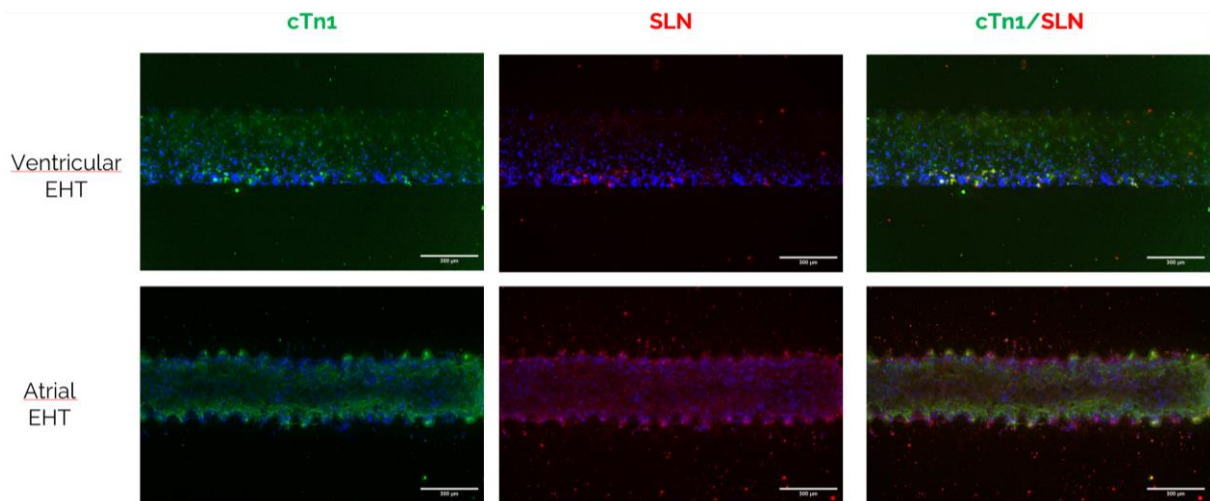


Figure 3.10: representative images of atrial (last three images) and ventricular (first three images) microtissues after 11 days of culturing in 3D in gel fibrin. Cardiac fibroblasts are identified by cardiac troponin I (red) and vimentin (green). Nuclei are stained with DAPI (blue).

4 Discussion

Globally, cardiovascular diseases (CVDs) are a significant cause of death, accounting for approximately 30% of all fatalities. These conditions involve issues with the vascular, cardiac, and nervous systems. The urgent need for new and improved medications and therapies to reduce the global burden of CVDs is paramount. The current treatment options for CVD mainly involve drugs that only slow down the disease progression. Despite advancements in drug development, heart transplantation remains the preferred method for treating heart disease due to its effectiveness. However, challenges such as donor shortages and the invasiveness of the surgery persist. To improve the drug development process, drug screening testing is essential. To overcome this, the heart-on-a-chip model has emerged as an innovative in vitro model that can recreate an in vivo-like environment for drug screening testing. By combining 3D structured models with mechanical or electrical stimulation, cell maturation can be enhanced, leading to more consistent outcomes in drug testing. This advancement in technology shows promise in improving the drug development process for CVD treatment.

This study conducted a comprehensive analysis of hiPSC atrial and ventricular microtissues on a 3D beating organ chip, focusing on mechanical, electrical, and biological features to provide a foundation for future drug screening studies. By analysing the data collected, significant differences were identified between atrial and ventricular cardiomyocytes from multiple perspectives. The study first examined the behaviour of the microtissues under static and dynamic conditions, finding that dynamic conditions consistently resulted in higher overall results compared to static conditions. Dynamic microtissues exhibited a stronger and more linear behaviour, as indicated by a higher Pearson's correlation coefficient and higher contraction amplitudes. The contraction amplitude augmentation from static to dynamic condition is linear with literature analysis, because the mechanical stimulation is able to improve the cell alignment, contractility properties and the electrical conduction velocity [28]. This Pearson's correlation coefficient behaviour was consistent with those of a previous thesis project of Mimic Lab, where it was found the same trend.

When focusing on dynamic conditions, atrial microtissues demonstrated a consistent beating period with increasing contraction amplitudes over time, while ventricular microtissues showed a slight decrease in beating period but an increase in contraction amplitude. Ventricular microtissues also displayed a more synchronized beating pattern compared to atrial microtissues except for the day 11 where the trend is inverted. This final day trend does find correlation with literature findings because atrial tissue tends to beat more rhythmically and regularly compared to ventricular

tissue. This is because the atria are responsible for initiating the electrical signal that triggers each heartbeat, whereas the ventricles mainly respond to this signal and contract in a coordinated manner [7].

Moreover, atrial dynamic microtissues exhibited a significantly higher contraction amplitude, especially in the later days of the study, contradicting previous literature that suggested ventricular microtissues should have greater, around 60% higher, strength due to myosin light chain isoform [29].

On the other hand, the overall mean beating period over the course of several days is higher for ventricular dynamic samples in comparison to atrial samples, which agrees with literature research. The time to peak remains consistent between the two sample types until day 8 and 11 when it is lower for atrial dynamic microtissues and this trend is confirmed by literature because the shortening velocity of atrial microtissues is higher than ventricular ones and this happens for their cross-bridge kinetics[9].

Meanwhile atrial dynamic samples consistently have longer relaxation times compared to ventricular samples, especially in the later days of the study and this goes in contradiction of the literature studies because atrial cardiomyocytes have a faster shortening velocity and relaxation than ventricular cardiomyocytes [14].

From the electrical characterization emerged variances in the electric activity between atrial and ventricular cardiomyocytes, where atrial samples exhibit greater spike amplitudes, quicker beating rhythms, and shorter field potential durations than ventricular ones. Additionally, the standard deviations for these parameters are generally lower in atrial samples, suggesting that atrial cardiomyocytes display more uniform electrical activity as opposed to ventricular cardiomyocytes.

In the literature, there is evidence regarding the field potential duration and beating period, while the results obtained concerning spike amplitude contradict previous findings [9]. This happens because the myofibrils density is lower in atrial cardiomyocytes than ventricular cardiomyocytes [9].

Subsequently, the biological characteristics of atrial and ventricular dynamic microtissues were examined. As anticipated, atrial microtissues exhibited high levels of sarcolipin, a protein specific to the atrial microtissues, while lacking the expression of ventricular myosin light chain-2, which is a specific ventricular protein. Conversely, ventricular microtissues showed elevated levels of ventricular myosin light chain-2 and did not express sarcolipin. This pattern of protein expression aligns with previous findings in the literature [27].

5 Conclusion and future developments

This study represents an essential step in understanding the differences in behaviour between atrial and ventricular cells on a 3D heart on a chip to establish a baseline for drug screening testing. To fully characterize the biological differences, previously started with the immunostaining, between the two types of cardiomyocytes, it will conduct PCR analysis to compare the gene expression levels of calcium, sodium, and potassium channels. This will provide insight into how variations in gene expression may contribute to differences in action potential shape, as previously observed in existing literature [9]. Moving forward, drug screening tests will be performed on day 8, being the day when the two kinds of microtissues reach their peaks. This will be crucial in determining how effective these treatments are in regulating the electrical and mechanical behaviour of the cardiomyocytes microtissues. By comparing the electrical and mechanical analysis of both cell types, it can better understand the effects of these drugs on the heart. The major limitation of the microfluidic device found in literature and the one used in this project is that they allow the study of just one singular cell kind at the time. The heart is made up of various regions, including atria and ventricles, each containing different types of cells. To accurately model the architecture of the heart, a new microfluidic design is required. Existing heart microfluidic devices, including the one used in this project, only allow for the culture of a single cell construct. To address this limitation, the ultimate objective of this project is to develop a new chip design that can support the co-culture of both atrial and ventricular cardiomyocytes. The design in question is a uStretch chip design composed by five channels, where the lateral ones are medium channels and the other three are done by atrial and ventricular channels divided by one channel made by endothelial cells and collagen. This layer should mimic the endocardium architecture which surrounds the valves which divides atrium from ventricle. In this way is possible to analyse a more complete model that better represent the full heart architecture. The innovative concept of simultaneously studying both types of cardiomyocytes in this research is a significant advancement that will enhance our understanding of the interplay between atrial and ventricular cells and could be used for drug screening testing to provide more complete data. The device is composed of five channels, two medium channels and three culture channels. Each culture channel is equipped with two 1mm diameter holes, one at the beginning and one at the end of the channel for injection inlet and outlet purposes. Additionally, each chamber presents four reservoirs for medium replacement with a 5 mm diameter. The three central channels measure 300 μm in width, 10mm in length, and 150 μm in height, with a 40 μm gap between pillars (Figure 5.1). The chip design includes four microelectrode channel guides two each side called recording guides, which allows

insertion of electrodes used to recording the field potential of atrial and ventricular microtissues. Overall, this study represents a significant advancement in cardiac research and has the potential to lead to more effective drug screenings and treatment options for heart conditions in the future.

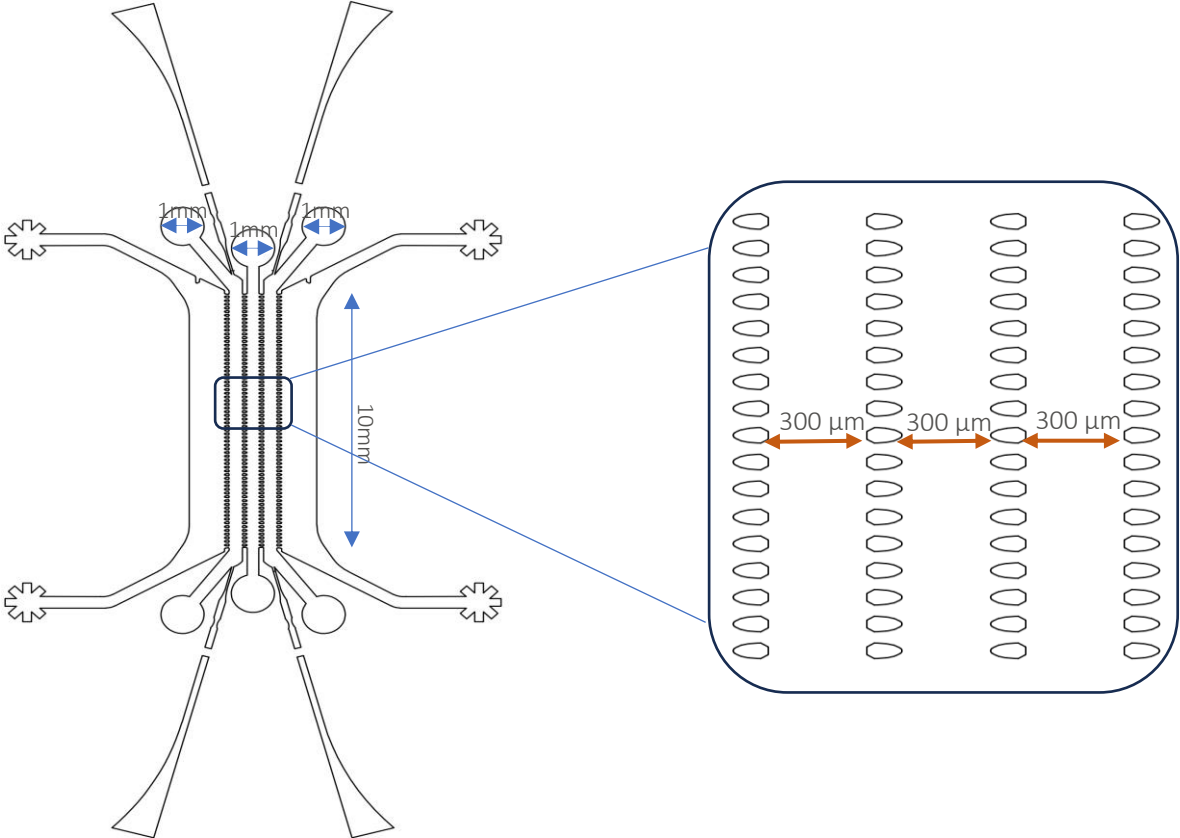


Figure 5.1: CAD design of a new microfluidic device which allows the co-culture of both atrial and ventricular microtissues on the extreme channels while in the middle one is reserve to a microtissue made by endothelial cells and collagen.

6 Bibliography

- [1] A. J. Weinhaus e K. P. Roberts, «Anatomy of the Human Heart», in *Handbook of Cardiac Anatomy, Physiology, and Devices*, P. A. Iaizzo, A c. di, Totowa, NJ: Humana Press, 2005, pp. 51–79. doi: 10.1007/978-1-59259-835-9_4.
- [2] S. Shah, G. Gnanasegaran, J. Sundberg-Cohon, e J. Buscombe, «The Heart: Anatomy, Physiology and Exercise Physiology», in *Integrating Cardiology for Nuclear Medicine Physicians: A Guide to Nuclear Medicine Physicians*, 2009, pp. 3–22. doi: 10.1007/978-3-540-78674-0_1.
- [3] E. Grandi *et al.*, «Diversity of cells and signals in the cardiovascular system», *J. Physiol.*, vol. 601, fasc. 13, pp. 2547–2592, lug. 2023, doi: 10.1113/JP284011.
- [4] W. Dun e P. A. Boyden, «The Purkinje cell; 2008 style», *J. Mol. Cell. Cardiol.*, vol. 45, fasc. 5, pp. 617–624, nov. 2008, doi: 10.1016/j.yjmcc.2008.08.001.
- [5] H. Hashimoto, E. N. Olson, e R. Bassel-Duby, «Therapeutic approaches for cardiac regeneration and repair», *Nat. Rev. Cardiol.*, vol. 15, fasc. 10, pp. 585–600, ott. 2018, doi: 10.1038/s41569-018-0036-6.
- [6] N. Anto Michel, S. Ljubojevic-Holzer, H. Bugger, e A. Zirlik, «Cellular Heterogeneity of the Heart», *Front. Cardiovasc. Med.*, vol. 9, p. 868466, 2022, doi: 10.3389/fcvm.2022.868466.
- [7] S. K. Padala, J.-A. Cabrera, e K. A. Ellenbogen, «Anatomy of the cardiac conduction system», *Pacing Clin. Electrophysiol. PACE*, vol. 44, fasc. 1, pp. 15–25, gen. 2021, doi: 10.1111/pace.14107.
- [8] F. Sheikh, R. S. Ross, e J. Chen, «Cell-cell connection to cardiac disease», *Trends Cardiovasc. Med.*, vol. 19, fasc. 6, pp. 182–190, ago. 2009, doi: 10.1016/j.tcm.2009.12.001.
- [9] S. Y. Ng, C. K. Wong, e S. Y. Tsang, «Differential gene expressions in atrial and ventricular myocytes: insights into the road of applying embryonic stem cell-derived cardiomyocytes for future therapies», *Am. J. Physiol.-Cell Physiol.*, vol. 299, fasc. 6, pp. C1234–C1249, dic. 2010, doi: 10.1152/ajpcell.00402.2009.

- [10] G. Schram, M. Pourrier, P. Melnyk, e S. Nattel, «Differential distribution of cardiac ion channel expression as a basis for regional specialization in electrical function», *Circ. Res.*, vol. 90, fasc. 9, pp. 939–950, mag. 2002, doi: 10.1161/01.res.0000018627.89528.6f.
- [11] Z. Kassiri, R. Hajjar, e P. H. Backx, «Molecular components of transient outward potassium current in cultured neonatal rat ventricular myocytes», *J. Mol. Med. Berl. Ger.*, vol. 80, fasc. 6, pp. 351–358, giu. 2002, doi: 10.1007/s00109-002-0325-7.
- [12] W. R. Giles e Y. Imaizumi, «Comparison of potassium currents in rabbit atrial and ventricular cells», *J. Physiol.*, vol. 405, pp. 123–145, nov. 1988, doi: 10.1113/jphysiol.1988.sp017325.
- [13] D. Fatkin, R. Otway, e J. Vandenberg, «Genes and Atrial Fibrillation A New Look at an Old Problem», *Circulation*, vol. 116, pp. 782–92, set. 2007, doi: 10.1161/CIRCULATIONAHA.106.688889.
- [14] N. Piroddi *et al.*, «Tension generation and relaxation in single myofibrils from human atrial and ventricular myocardium», *Pflugers Arch.*, vol. 454, fasc. 1, pp. 63–73, apr. 2007, doi: 10.1007/s00424-006-0181-3.
- [15] J. van der Velden *et al.*, «Isometric tension development and its calcium sensitivity in skinned myocyte-sized preparations from different regions of the human heart», *Cardiovasc. Res.*, vol. 42, fasc. 3, pp. 706–719, giu. 1999, doi: 10.1016/s0008-6363(98)00337-x.
- [16] G. A. Roth *et al.*, «Global Burden of Cardiovascular Diseases and Risk Factors, 1990–2019: Update From the GBD 2019 Study», *J. Am. Coll. Cardiol.*, vol. 76, fasc. 25, pp. 2982–3021, dic. 2020, doi: 10.1016/j.jacc.2020.11.010.
- [17] Y. Zhao *et al.*, «Towards chamber specific heart-on-a-chip for drug testing applications», *Adv. Drug Deliv. Rev.*, vol. 165–166, pp. 60–76, gen. 2020, doi: 10.1016/j.addr.2019.12.002.
- [18] M. Campbell, M. Chabria, G. A. Figtree, L. Polonchuk, e C. Gentile, «Stem Cell-Derived Cardiac Spheroids as 3D In Vitro Models of the Human Heart Microenvironment», in *Stem Cell Niche: Methods and Protocols*, K. Turksen, A c. di, New York, NY: Springer, 2019, pp. 51–59. doi: 10.1007/7651_2018_187.
- [19] I. R. Suhito e T.-H. Kim, «Recent advances and challenges in organoid-on-a-chip technology», *Organoid*, vol. 2, p. e4, apr. 2022, doi: 10.51335/organoid.2022.2.e4.
- [20] J. Veldhuizen, J. Cutts, D. A. Brafman, R. Q. Migrino, e M. Nikkhah, «Engineering anisotropic human stem cell-derived three-dimensional cardiac tissue on-a-chip», *Biomaterials*, vol. 256, p. 120195, ott. 2020, doi: 10.1016/j.biomaterials.2020.120195.
- [21] F. Zhang *et al.*, «Design and fabrication of an integrated heart-on-a-chip platform for construction of cardiac tissue from human iPSC-derived cardiomyocytes and *in situ* evaluation of physiological function», *Biosens. Bioelectron.*, vol. 179, p. 113080, mag. 2021, doi: 10.1016/j.bios.2021.113080.

- [22] A. Marsano *et al.*, «Beating heart on a chip: a novel microfluidic platform to generate functional 3D cardiac microtissues», *Lab. Chip*, vol. 16, fasc. 3, pp. 599–610, gen. 2016, doi: 10.1039/C5LC01356A.
- [23] R. Visone *et al.*, «A microscale biomimetic platform for generation and electro-mechanical stimulation of 3D cardiac microtissues», *APL Bioeng.*, vol. 2, fasc. 4, p. 046102, dic. 2018, doi: 10.1063/1.5037968.
- [24] R. Visone *et al.*, «Micro-electrode channel guide (μ ECG) technology: an online method for continuous electrical recording in a human beating heart-on-chip», *Biofabrication*, vol. 13, fasc. 3, p. 035026, lug. 2021, doi: 10.1088/1758-5090/abe4c4.
- [25] L. Sala *et al.*, «MUSCLEMOTION», *Circ. Res.*, vol. 122, fasc. 3, pp. e5–e16, feb. 2018, doi: 10.1161/CIRCRESAHA.117.312067.
- [26] R. Visone *et al.*, «Predicting human cardiac QT alterations and pro-arrhythmic effects of compounds with a 3D beating heart-on-chip platform», *Toxicol. Sci.*, vol. 191, fasc. 1, pp. 47–60, ott. 2022, doi: 10.1093/toxsci/kfac108.
- [27] I. Goldfracht *et al.*, «Generating ring-shaped engineered heart tissues from ventricular and atrial human pluripotent stem cell-derived cardiomyocytes», *Nat. Commun.*, vol. 11, p. 75, gen. 2020, doi: 10.1038/s41467-019-13868-x.
- [28] B. Gu *et al.*, «Heart-on-a-chip systems with tissue-specific functionalities for physiological, pathological, and pharmacological studies», *Mater. Today Bio*, vol. 24, p. 100914, feb. 2024, doi: 10.1016/j.mtbio.2023.100914.
- [29] H. Yamashita *et al.*, «Myosin light chain isoforms modify force-generating ability of cardiac myosin by changing the kinetics of actin-myosin interaction», *Cardiovasc. Res.*, vol. 60, fasc. 3, pp. 580–588, dic. 2003, doi: 10.1016/j.cardiores.2003.09.011.

List of Figures

Figure 1.1: Comparison between ventricular action potential (dotted line) and atrial action potential (solid line). Ventricular action potential exhibits a less negative resting potential, a shortened plateau phase, and a slower terminal repolarization respect atrial one. Take from [13]	3
Figure 1.2: number of deaths through the years for CVD diseases. Adapted from [16]	4
Figure 1.3: Schematic representation of the microfluidic device. The culture chamber is confined by trapezoidal micropillars, while the central part is patterned with an array of microposts that stimulate the cardiac tissue maturation. Adapted from [20]	6
Figure 1.4: Platform made by three assembled PDMS layers bonded to a glass surface. (i) Top layer with four inlet/outlet holes, (ii) channel layer, (iii) layer with two parallel platinum (Pt) wire electrodes embedded at the bottom, (iv) bottom layer: glass plated with four gold electrodes (a). Three – dimensional schematic drawing (b). Cross – section of the device showing the distribution of cells within the device (c). Detailed design of the channel layer (ii) (d). Image of the assembled microfluidic device (e). Taken from [21]	6
Figure 1.5: heart on a chip composed by two compartmentalized separated by a PDMS layer. The central channel is filled with cell laden fibrin gel (a). The construct is repeatedly stimulated by exerting pressure on the lower compartment, causing the PDSM membrane to bend (b). The final device is achieved through the permanent bonding of three distinct PDMS layers (c). A 3D sketch of the microfluidic platform (d). Device photograph (e). Cross – sectional characterization of the device (f). Taken from [22]	7
Figure 1.6: Electrical stimulation with two stainless steel electrodes inserted in parallel with the cell construct. Taken from [23].....	7
Figure 1.7: uHeart platform combining μ ECG technology with our existing beating heart on chip design. The uHeart platform is designed with a cell culture layer that includes three individual cell culture chambers (highlighted in red). Within each chamber, there is a 3D microtissue and two microguides for electrode insertions (highlighted in blue). The cell culture layer is intended to be connected to a single actuation layer (highlighted green) that delivers mechanical stimulation to all three microtissues at the same time (a). Inside the device, each cell culture chamber (1, 2, 3) is placed directly above its corresponding actuation chamber, which is sealed at the bottom with a cover slide for visual examination (b). Adapted from [24]	8
Figure 2.1: uStretch [®] platform produced by BiomimX [®] S.r.l	11
Figure 2.2 microfluidic one chamber CAD design of one top layer with a focus on the pillars shape. ...	12
Figure 2.3: schematic representation of the uStretch cross-section in rest (picture on the right) and in actuation phase. Adapted from [22].....	12

Figure 2.4: uBOX platform (BiomimX s.r.l.), which is a control system able to provide mechanical stimulation to each uStretch® platform.....	13
Figure 2.5: resin uStretch mold.....	14
Figure 2.6: silicon actuation wafer already poured with PDMS	14
Figure 2.7: mechanical set up for uStretch testing with a 0.7 Bar pressure for at least 30 minutes. ...	15
Figure 2.8: microscopic view of the electrode injection through μ ECG line	16
Figure 2.9: protocol followed for the mechanical characterization analysis and video recording	20
Figure 2.10: protocol followed for the electrical characterization analysis and video recording	20
Figure 2.11: three ROIs taken from one microtissue for MuscleMotion analysis.....	21
Figure 2.12: recorded ECG signal showing the three parameters of interest, which are the beating period, spike amplitude and field potential duration.....	22
Figure 2.13: schematic representation about the electric set-up acquisition system.	23
Figure 3.1: comparison between dynamic and static condition for both atrial (red dots) and ventricular (black dots) microtissues. Statistical test performed to obtain statistical significance (** $P < 0.001$ and * $P < 0.01$).	26
Figure 3.2: on the left histogram there is the correlation coefficient comparison between dynamic samples and on the right histogram between static ones.	26
Figure 3.3: graphs showing beating period, contraction amplitude, time to peak and relaxation time for atrial dynamic microtissues (red dots), from day 5 to day 11 of culturing, and ventricular dynamic microtissues (black dots). Statistical test performed to obtain statistical significance (** $P < 0.0001$, *** $P < 0.001$, ** $P < 0.01$ and * $P < 0.05$).	27
Figure 3.4 graphs showing comparisons between atrial and ventricular dynamic microtissues for beating period, contraction amplitude, relaxation time and time to peak though the days of culturing. Statistical test performed to obtain statistical significance (** $P < 0.001$, ** $P < 0.01$ and not significant (ns) with a $P > 0.05$).	28
Figure 3.5: graphs showing comparisons between atrial and ventricular static microtissues for beating period, contraction amplitude, relaxation time and time to peak though the days of culturing. Statistical test performed to obtain statistical significance (ns with $P > 0.05$).	29
Figure 3.6: spike amplitude comparison between atrial and ventricular samples at day 11 of culturing. Statistical test performed to obtain statistical significance (ns with $P > 0.05$).	30
Figure 3.7: beating period, field potential duration and field potential duration after Fridericia's correction comparison between atrial and ventricular samples after 11 day of culturing. Statistical test performed to obtain statistical significance (ns with $P > 0.05$).	31
Figure 3.8: representative images of atrial (last three images) and ventricular (first three images) microtissues after 11 days of culturing in 3D in gel fibrin. Cardiac fibroblasts are identified by cardiac troponin I (green), ventricular cardiomyocytes by ventricular myosin light chain 2 (red) and atrial cardiomyocytes are not stained because they don't express myosin light chain ventricular being a specific ventricular marker. Nuclei are stained with DAPI (blue).	32

Figure 3.9 : representative images of atrial (last three images) and ventricular (first three images) microtissues after 11 days of culturing in 3D in gel fibrin. Cardiac fibroblasts are identified by cardiac troponin I (green), atrial cardiomyocytes by sarcolipin (red) and ventricular cardiomyocytes are not stained because they don't express sarcolipin being a specific atrial marker. Nuclei are stained with DAPI (blue).....33

Figure 3.10: representative images of atrial (last three images) and ventricular (first three images) microtissues after 11 days of culturing in 3D in gel fibrin. Cardiac fibroblasts are identified by cardiac troponin I (red) and vimentin (green). Nuclei are stained with DAPI (blue).33

Figure 5.1: CAD design of a new microfluidic device which allows the co-culture of both atrial and ventricular microtissues on the extreme channels while in the middle one is reserve to a microtissue made by endothelial cells and collagen.37

List of Tables

Non è stata trovata alcuna voce dell'indice delle figure.

List of symbols

Variable	Description	SI unit
u	solid displacement	m
u_f	fluid displacement	m

Acknowledgments

